

THE UNIVERSITY OF MICHIGAN
INDUSTRY PROGRAM OF THE COLLEGE OF ENGINEERING

SCREENING OF SURFACE WAVES IN SOILS

Richard D. Woods

January, 1968

IP-804

ACKNOWLEDGMENTS

The author wishes to acknowledge and thank the National Science Foundation for the support provided for this investigation. The research represents part of the study being conducted under NSF GP-342 and GK-1208. These grants provided for the assistance required for conducting the tests and for preparing this paper. During the course of this study, the author was supported through the NSF Graduate Traineeship Program.

This paper represents a portion of a PH.D. dissertation prepared by the author in the Department of Civil Engineering at the University of Michigan. The author wishes to thank Professor F. E. Richart, Jr., chairman of the doctoral committee and Professors G. V. Berg, J. R. Hall, Jr., I. K. McIvor, and H. N. Pollack, committee members, for their advice, encouragement, and editorial help in preparing the dissertation and this paper.

Further appreciation is extended to the author's colleagues in the soil dynamics group, particularly Dr. V. P. Drnevich for his stimulating interest, and to K. H. Stokoe and M. G. Katona for their help in performing the tests and preparing illustrations.

TABLE OF CONTENTS

	<u>Page</u>
ACKNOWLEDGMENTS.....	iii
LIST OF TABLES.....	vii
LIST OF FIGURES.....	ix
INTRODUCTION.....	1
SEISMIC WAVES IN AN ELASTIC HALF SPACE.....	2
SCATTERING AND DIFFRACTION OF ELASTIC WAVES.....	7
EXPERIMENTAL APPROACH AND GENERAL PROCEDURES.....	8
DESCRIPTION OF TEST LAYOUT, INSTRUMENTATION AND FIELD SITE..	13
ACTIVE ISOLATION TESTS.....	20
PASSIVE ISOLATION TESTS.....	39
CONCLUSIONS.....	51
Appendix I - REFERENCES.....	54
Appendix II - LIST OF SYMBOLS.....	56

LIST OF TABLES

<u>Table</u>		<u>Page</u>
I	Wave Length and Wave Velocity for the Rayleigh Wave at the Field Site.....	22
II	Schedule of Field Tests for Active Isolation.....	23
III	Active Isolation Tests with Trench Length θ , 360° and Trench Radius, R_0 , 1.0 Foot.....	30
IV	Active Isolation Tests with Trench Length θ , 360° and Trench Radius, R_0 , 0.5 Foot.....	32
V	Distance from the Source of Vibration to the "Principal Minimum" (in Wave Lengths) for Full Circle Active Isolation Tests.....	38
VI	Schedule of Field Tests for Passive Isolation.....	41
VII	Shallowest Trenches which Satisfied Screening Criteria in Passive Isolation Tests.....	45
VIII	List of Tests Using Sheet-Wall Barriers.....	50

LIST OF FIGURES

<u>Figure</u>		<u>Page</u>
1	Distribution of Displacement Waves from a Circular Footing on a Homogeneous, Isotropic, Elastic Half Space.....	4
2	Schematic of Vibration Isolation using a Circular Trench Surrounding the Source of Vibrations-- Active Isolation.....	9
3	Schematic of Vibration Isolation using a Straight Trench to Create a Quiescent Zone-- Passive Isolation.....	10
4	Photograph of Field Site.....	14
5	Field Site Soil Properties and Schematic of Instrumentation.....	16
6	Grain Size Distribution Curves--Field Site Soils....	17
7	Mohr's Circle Diagram for Drained Triaxial Tests on Undisturbed Samples (Upper Layer).....	18
8	Schematic of Test Layout for Active Isolation in the Field.....	21
9	Photograph of Field Test Layout for Isolation at the Source.....	25
10	Amplitude Reduction Factor versus Distance from Source--Three Tests.....	26
11	Amplitude Reduction Factor Contour Diagram, Test AF-7-300.....	27
12	Amplitude Reduction Factor Contour Diagram, Test AF-5-300.....	28
13	Amplitude Reduction Factor Contour Diagram, Test AF-6-300.....	29
14	Amplitude Reduction Factor Contour Diagram, Test AF-3-250.....	34
15	Amplitude Reduction Factor Contour Diagram, Test AF-4-300.....	35

LIST OF FIGURES (CONT'D)

<u>Figure</u>		<u>Page</u>
16	Amplitude Reduction Factor versus Distance from Source--Location of "Principal Minimum".....	37
17	Plan View of Field Site Layout for Screening at a Distance.....	40
18	Amplitude Reduction Factor Contour Diagram, Test PF-12-250.....	43
19	Amplitude of Vertical Displacement versus Distance from Source for Five Tests.....	44
20	Amplitude Reduction Factor Contour Diagram, Test PF-17-250.....	47
21	Amplitude Reduction Factor Contour Diagram, Test PF-21-250.....	48
22	Amplitude Reduction Factor Contour Diagram, Test SF-6-250.....	49

INTRODUCTION

Trenches and sheet-pile walls have been used for many years in attempts to isolate foundations of machines and structures from vibratory energy but have not always been successful. Barkan (1962) stated, after reviewing many applications of trenches and sheet-pile barriers in isolation problems, "Experience with various barriers has shown that they are often of no use at all or their effect is very small." The reason for this frequent lack of success was postulated by Barkan as he went on to state that in the cases where barriers were of no use the designers did not adequately account for or did not adequately understand the theory of surface wave propagation in the presence of a barrier. It is evident that a rational design approach based on a thorough understanding of surface waves in the region of obstacles must be available if foundation isolation systems incorporating trench or sheet-wall barriers are to be employed with confidence. Currently there is insufficient theoretical and empirical knowledge on which to base a design approach. The objective of the research described herein was to obtain basic information on the screening of elastic surface waves by trench barriers from which a rational design approach might eventually be derived.

SEISMIC WAVES IN AN ELASTIC HALF SPACE

An understanding of the phenomena associated with elastic wave propagation in a half space is of fundamental importance in studying the isolation of foundations by barriers. The energy which causes ground motion or footing motion is transmitted through the earth by elastic displacement waves, seismic waves. In the analysis of seismic wave propagation, it is common to assume that the earth can be simulated by a homogeneous, isotropic, elastic half space. This assumption is made frequently in seismology and in many soil mechanics problems concerning stress at a point in a soil medium.

There is an abundance of information relative to the propagation of seismic waves in a homogeneous, isotropic, elastic half space; Lamb (1904), Kolsky (1953), Ewing, Jardetzky and Press (1957), Grant and West (1965) and others. Elastic half space theory defines two basic types of waves, body waves and surface waves. There are two important body waves, the compression wave (P-wave) and the shear wave (S-wave), and there is one surface wave, the Rayleigh wave (R-wave).

Elastic waves may originate in many ways; from earthquake explosions, pile driving operations, or vibrating machine footing. The source of elastic waves may be contained within the half space or may be on its surface. Since most footings for buildings and machinery are located on or near the surface of the earth, seismic waves generated by surface sources are of primary interest in foundation isolation studies. The energy coupled into the soil by a surface is transmitted away from the source by a combination of P, S, and R-waves. The distribution of energy among these waves has been computed by Miller and Pursey

(1955) for the case of an elastic half space having a Poisson's ratio of $1/4$, ($\nu = 1/4$), excited by a vertically oscillating circular disk. The basic features of wave propagation in a half space and of Miller and Pursey's energy partition calculations are shown on Figure 1. This figure should be used as a reference for the following discussion of elastic wave propagation.

On Figure 1 it is shown that body waves propagate radially outward from the source along hemispherical wave fronts and that the Rayleigh wave propagates radially outward on a cylindrical wave front. All of the waves encounter an increasingly larger volume of material as they travel outward; thus the energy density in each wave decreases with distance from the source. This decrease in energy density or decrease in displacement amplitude is called geometrical damping. The geometrical damping law governing body waves is expressed by $1/r$ (except along the surface where it is $1/r^2$), and the geometrical damping law for the Rayleigh wave is given by $1/r^{0.5}$. The particle motion associated with the compression wave is a push-pull motion in the direction of the wave front, the particle motion associated with the shear wave is a transverse displacement normal to the direction of the wave front, and the particle motion associated with the Rayleigh wave at the surface of a half space is a retrograde ellipse. The shaded zones along the wave fronts for the body waves indicate the relative amplitude of particle displacement as a function of the dip angle (the angle measured downward from the surface at the center of the source). The Rayleigh wave can be described by two components, vertical and horizontal, each of which decays with depth but according to separate distributions.

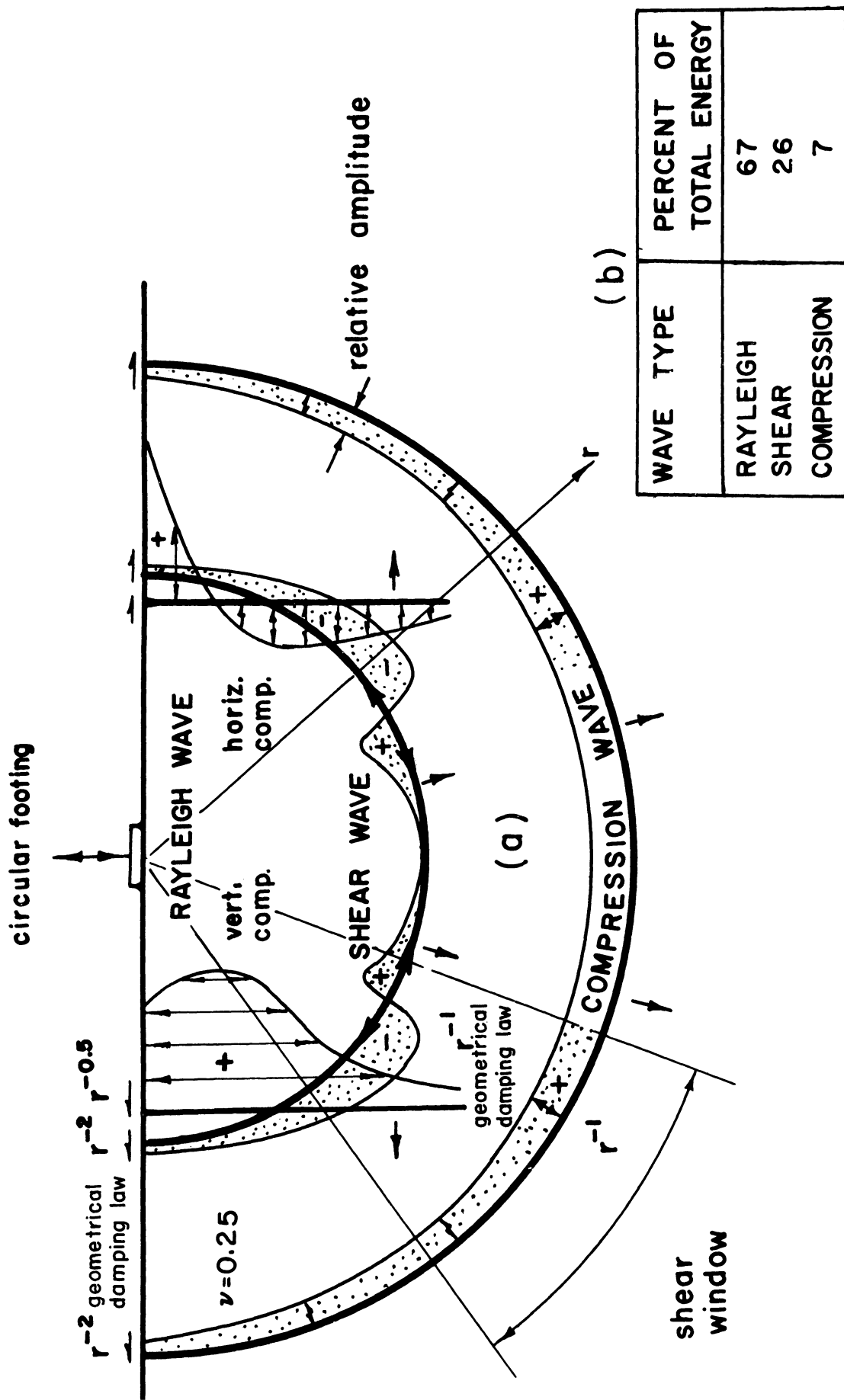


Figure 1. Distribution of Displacement Waves from a Circular Footing on a Homogeneous, Isotropic, Elastic Half Space.

For a vertically oscillating circular energy source on the surface of a homogeneous, isotropic, elastic half space, Miller and Pursey (1955) determined the distribution of total input energy among the three elastic waves to be: 67 percent Rayleigh wave, 26 percent shear wave, and 7 percent compression wave. The facts that 2/3 of the total input energy is transmitted away from a surface energy source by the Rayleigh wave and that the Rayleigh wave decays much more slowly with distance than the body waves indicate that the Rayleigh wave is of primary concern for foundation isolation problems.

The distance from the source of waves to each wave front on Figure 1 is drawn in proportion to the velocity of each wave. The expressions for wave velocity are as follows:

P-wave, v_P ,

$$v_P = \sqrt{\frac{\lambda + 2G}{\rho}}$$

where λ and G are Lamé's constants (G is also known as the shear modulus), ρ is the mass density of the material ($\rho = \gamma/g$ where γ is the unit weight and g is 32 foot/second²), ν = Poisson's ratio, and $\lambda = \frac{2\nu G}{1 - 2\nu}$,

S-wave, v_S ,

$$v_S = \sqrt{\frac{G}{\rho}} , \text{ and}$$

R-wave, v_R ,

$$v_R = k v_S$$

where k is a constant ($0.874 \leq k \leq 0.955$) depending on Poisson's ratio, and for the values of Poisson's ratio appropriate for soils, v_R and v_S are very nearly the same and for practical purposes are often considered identical.

SCATTERING AND DIFFRACTION OF ELASTIC WAVES

The preceding discussion pertained only to an unobstructed, homogeneous, isotropic half space where elastic waves did not encounter barriers of any kind. The concept of footing isolation by trenches or sheet-pile walls, however, is dependent on the interception, scattering and diffraction of surface waves by barriers. Theoretical solutions for diffraction and scattering of body waves in elastic media by cylinders and spheres have been presented by Tyutekin (1959), Knopoff (1959) and Baron and Matthews (1961). Two-dimensional theoretical and experimental studies of the reflection and transmission of surface waves by step changes in elevation, corners and notches have been presented by Mal and Knopoff (1965), Viktorov (1958), and deBremaecker (1958); however, a theory describing the diffraction and scattering of surface waves by obstacles of finite dimensions is not currently available. This pinpoints the area where further study is required to improve the art of footing isolation by trenches, namely, the screening effects of three-dimensional obstacles at the surface of a half space.

EXPERIMENTAL APPROACH AND GENERAL PROCEDURES

There are two basic approaches which could be followed in studying the problem of screening of elastic waves by trenches or other barriers, theoretical and experimental. The theoretical approach was not encouraging due to the mathematical complexities of this problem so the experimental approach was pursued. From a practical standpoint an extensive series of full-scale footing isolation tests was not feasible; so the model approach was investigated. The model approach has been used extensively in seismological studies as described by Northwood and Anderson (1953) and Oliver, Press and Ewing (1954), and, furthermore, Lysmer and Richart (1966) have shown through dimensionless analysis that wave length scaling is appropriate for footing vibration problems. Thus, it was concluded that the model approach was appropriate for the footing isolation problem and that pertinent dimensions of the barriers could be evaluated in terms of the wave length of the Rayleigh wave.

When studying the screening of elastic waves by trenches, it is convenient to subdivide the problem into two categories, (1) active isolation (isolation at the source) and (2) passive isolation (screening at a distance). Active isolation, as shown schematically on Figure 2, is the employment of barriers close to or surrounding the source of vibrations to reduce the amount of wave energy radiated away from the source. Passive isolation, as shown schematically in Figure 3, is the employment of barriers at points remote from the source of vibrations but near a site where the amplitude of vibration must be reduced. Both types of foundation isolation problems were investigated.

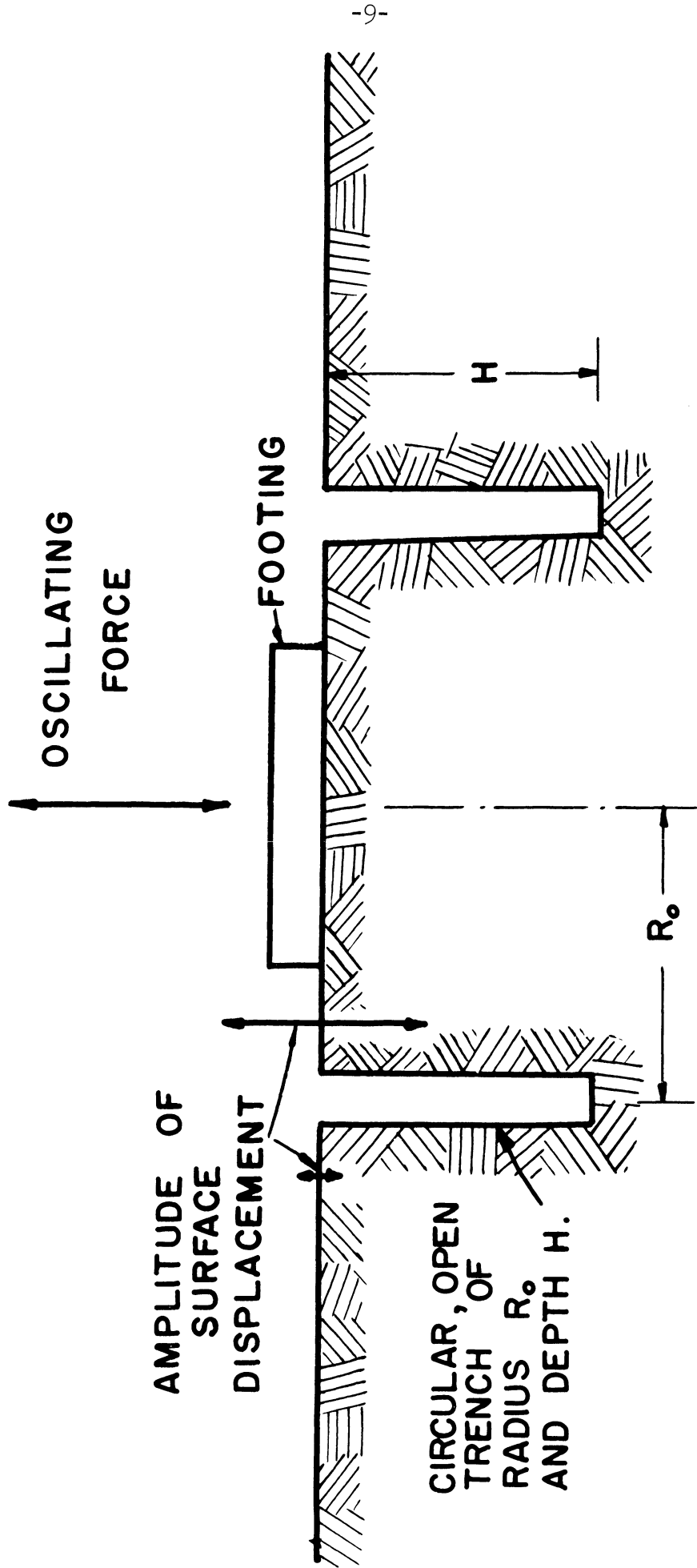


Figure 2. Schematic of Vibration Isolation Using a Circular Trench Surrounding the Source of Vibrations--Active Isolation.

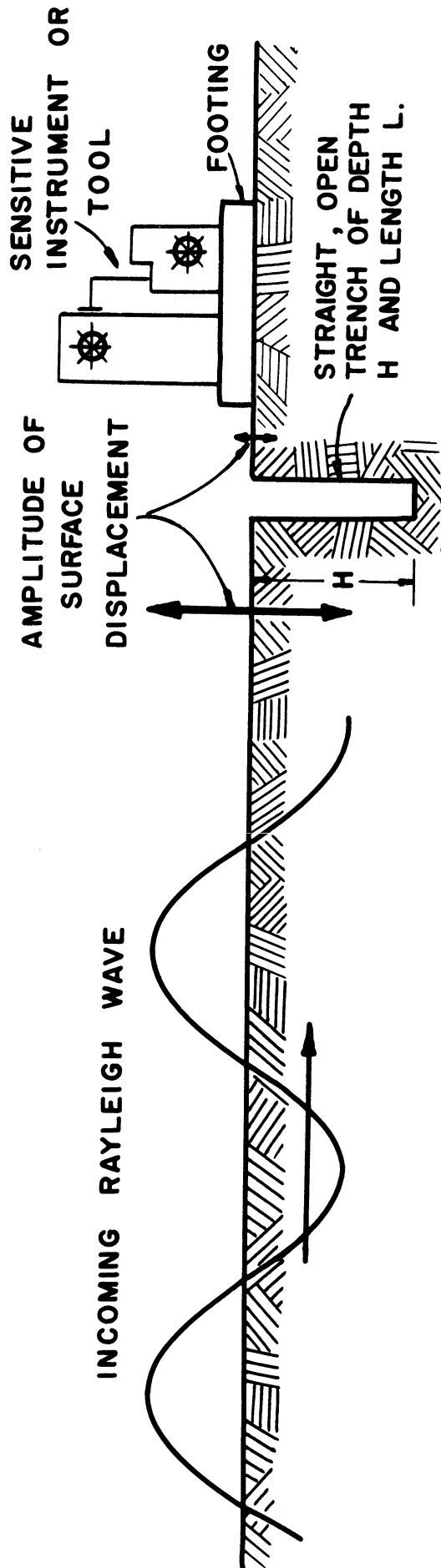


Figure 3. Schematic of Vibration Isolation Using a Straight Trench to Create a Quiescent Zone--Passive Isolation.

The general purpose of this research was to define the screening effects of trench barriers, and the specific purpose was to define the screened zone and degree of amplitude reduction within the screened zone for trenches of a few specific shapes and sizes. It was anticipated that a threshold trench size could be established below which trenches would have little effectiveness, and the results tend to confirm this concept.

The general plan for the footing isolation tests was (1) to set up a source of vibration at the center of a prepared site, (2) to determine the amplitude of vertical ground motion at selected points throughout the test site for the "no trench" or before conditions, (3) to dig a trench barrier, and (4) to determine the amplitude of ground motion at the same selected points for the after condition. A comparison of before and after conditions provided the means of evaluating the effectiveness of the barrier. For each pickup point a ratio, called the "amplitude reduction factor," relating amplitude after trench installation to amplitude before trench installation was computed. This ratio gave a quantitative evaluation of the effect of the trench on the amplitude of vertical ground motion at each pickup point.

The data accumulated in tests as described above was displayed for evaluation in two ways. The first was to plot amplitude of vertical ground motion versus distance from the source for vibration measurements along a radius from the source of vibrations and through a point of symmetry on the trench. When curves of this type for several trench sizes were drawn on the same chart, a direct comparison of the effectiveness of the various trenches was possible. This type of plot,

however, gave no information on the lateral extent of trench effectiveness and did not indicate the shape of the screened zone. A second method of displaying the data was employed in which "amplitude reduction factors" were plotted for each pickup point on a plan diagram of the test layout and contours of equal "amplitude reduction factor" were drawn. The amplitude reduction factor contour diagrams provided the means for evaluating the lateral extent and the shape of the second zone.

Two criteria were established from which the relative effectiveness of the various trenches was evaluated. One criterion specified the amplitude reduction, and the other specified the area in which the amplitude reduction had to be effective. The amplitude reduction criterion for all tests was an amplitude reduction factor of 0.25. But, due to the differences in overall geometry of active isolation tests and passive isolation tests, separate area criteria were necessary. The area criterion for active isolation with 360° trenches specified that 75 percent of the area of the test site beyond the barrier had to be enclosed by an amplitude reduction factor contour of 0.25 or less. For trenches of less than 360° an additional area criterion was necessary and will be described in a later paragraph. The area criterion for passive isolation specified that 75 percent of a semicircular area with center at the mid-point of the trench and radius equal to one half the trench length had to be enclosed by an amplitude reduction factor contour of 0.25 or less.

DESCRIPTION OF TEST LAYOUT, INSTRUMENTATION AND FIELD SITE

Each test layout consisted of a vibration exciter as the source of input motion, a trench to screen displacement waves, and pickup points at which to measure the amplitude of vertical ground motion. Early in the testing program it became evident that special provisions would be required to obtain repeatable ground motion measurements at each pickup point. Several methods were tried for obtaining repeatable measurements, and the most successful method was to provide a small steel plate, 2 inch by 2 inch by 1/4 inch, at each pickup point, set in the ground with its top surface flush with the soil surface. These steel plates were called pickup benches. Ground motion measurements were made by placing a motion transducer on each pickup bench in succession.

The vibration source was an MB Electronics Model C-31 vibration exciter weighing about 73 pounds. A constant input excitation force of 18 pounds (vector force) was used in all tests. At this force level the exciter displacement was about 20 microns.

An MB Electronics power amplifier, oscillator and field supply unit was used to drive the vibration exciter. Surface motion measurements were made with an Electro-Tech vertical velocity transducer. A Tektronix 502 dual beam oscilloscope and a Hewlett-Packard 427A voltmeter were used to monitor the input motion of the exciter and to measure the transducer output.

The selected field site, shown in Figure 4, was situated on a sand and silt deposit in an area remote from sources of man-made seismic noise. A profile showing the pertinent properties of the soil

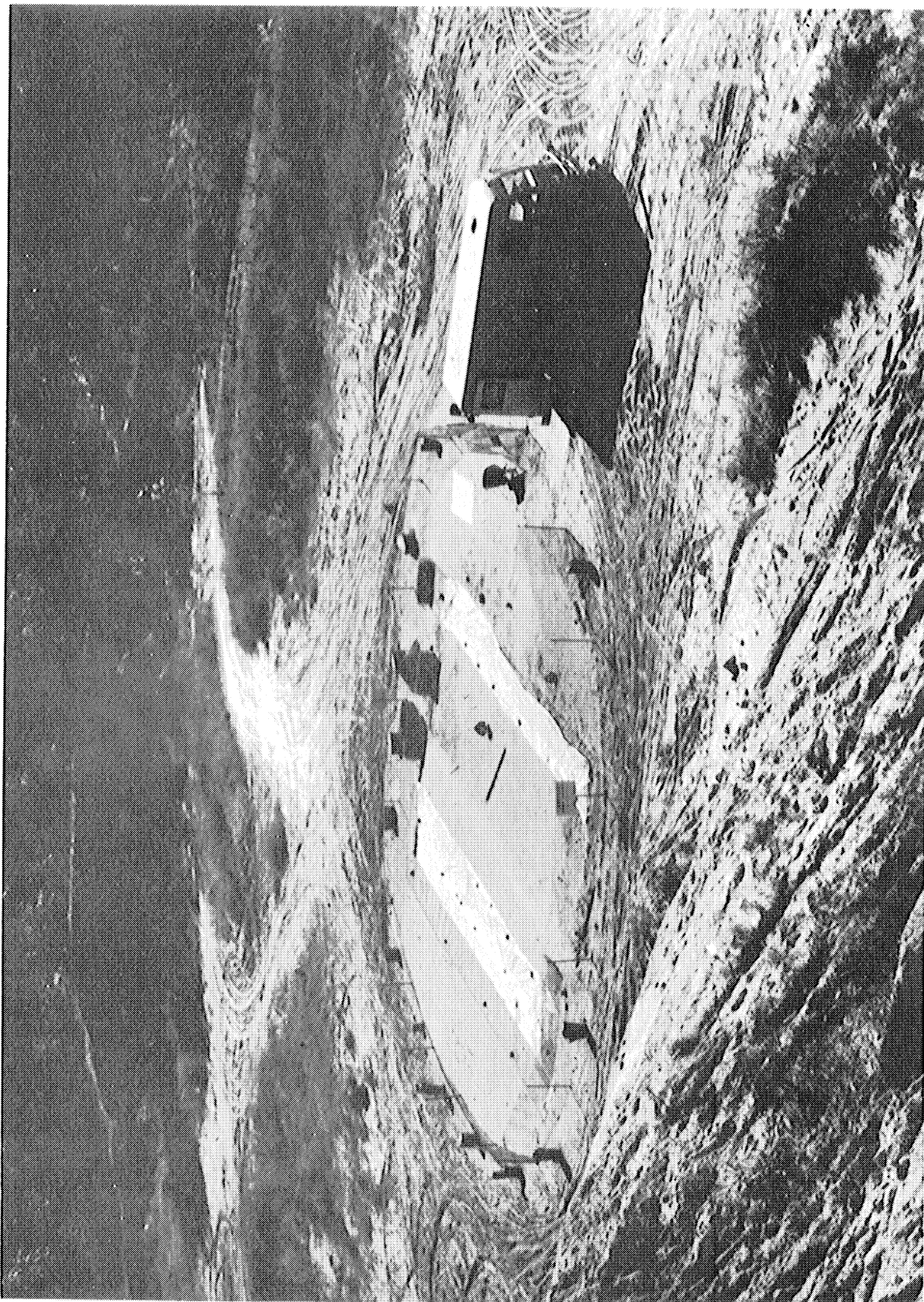


Figure 4. Photograph of Field Site.

at the selected site is shown in Figure 5. This profile shows a two-layer system, and the grain size distribution for the soil of each layer is shown on Figure 6. A water table was not located in hand borings to a depth of 14 feet or in refraction surveys of the site.

Drained triaxial compression tests were performed on undisturbed samples from the upper layer to determine the $c-\phi$ characteristics of the soil. A Mohr's circle diagram for the triaxial tests is shown on Figure 7. The angle of internal friction, ϕ , was 38° and the cohesion intercept, c , was 0.35 kg/cm^2 . In a moist condition, $w = 5$ percent to 15 percent, this soil maintained vertical-walled open trenches up to four feet deep.

An area about 75 feet in diameter, shown on Figure 4, was fenced, and its surface was leveled and compacted with a Jackson vibratory compactor. After a gentle rainfall had thoroughly moistened the surface, a circular area 25 feet in diameter was carefully prepared by tamping with a hand tamper and leveling with a straight edge. Surface preparation in the test area was considered very important for two reasons: (1) the edges of the trenches at the surface would be vulnerable to crumbling and shear failure, therefore the strength of the soil at the surface should be as great as possible, and (2) the soil near the surface had to be uniform and compact so that pickup benches placed on the soil surface would reproduce true vertical motion response. The prepared area was covered with a plastic film to prevent moisture loss at all times except during the performance of a test. The plastic film also helped to create a uniform distribution of moisture within the zone at the test site which it covered.

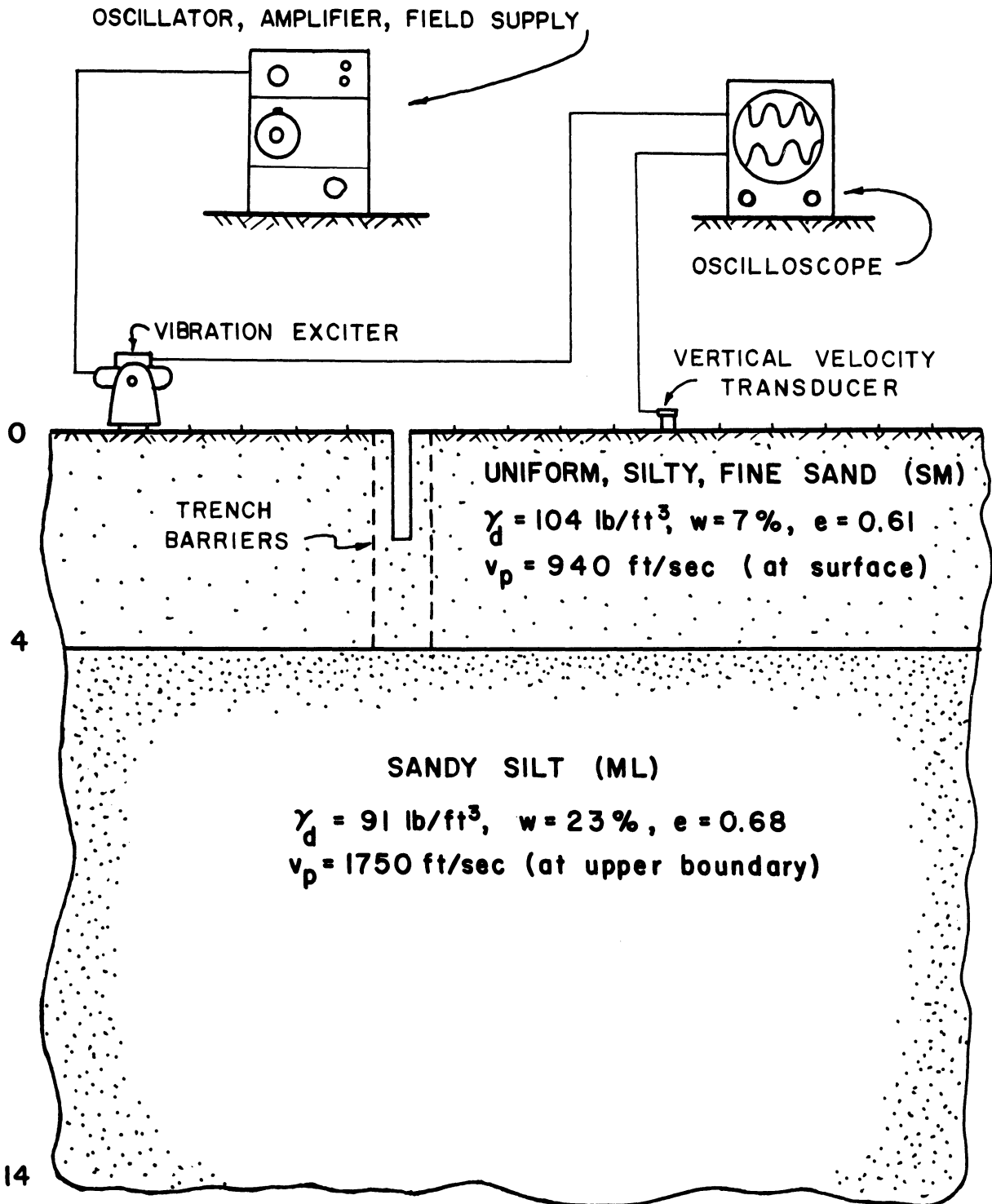


Figure 5. Field Site Soil Properties and Schematic of Instrumentation.

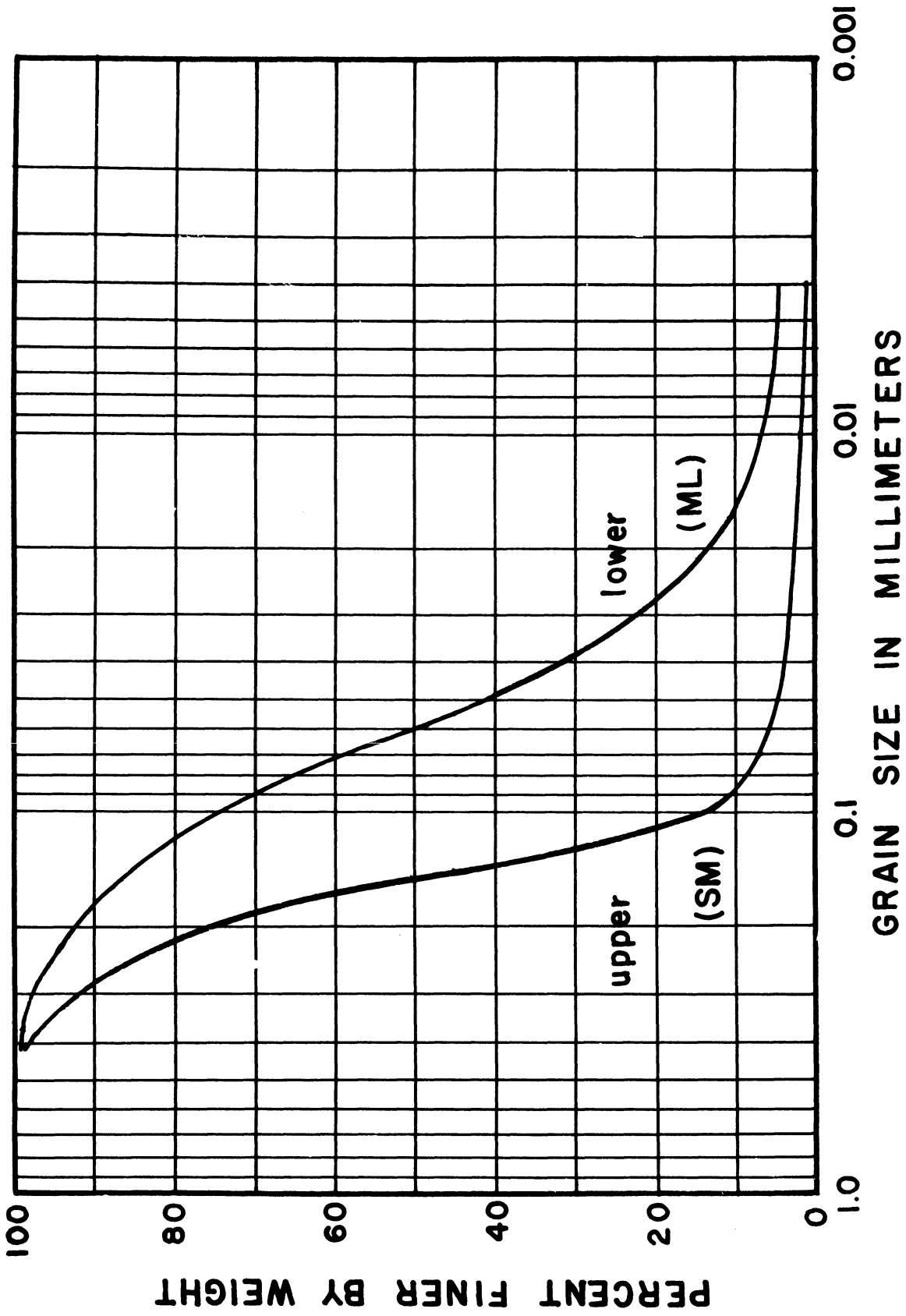


Figure 6. Grain Size Distribution Curves--Field Site Soils.

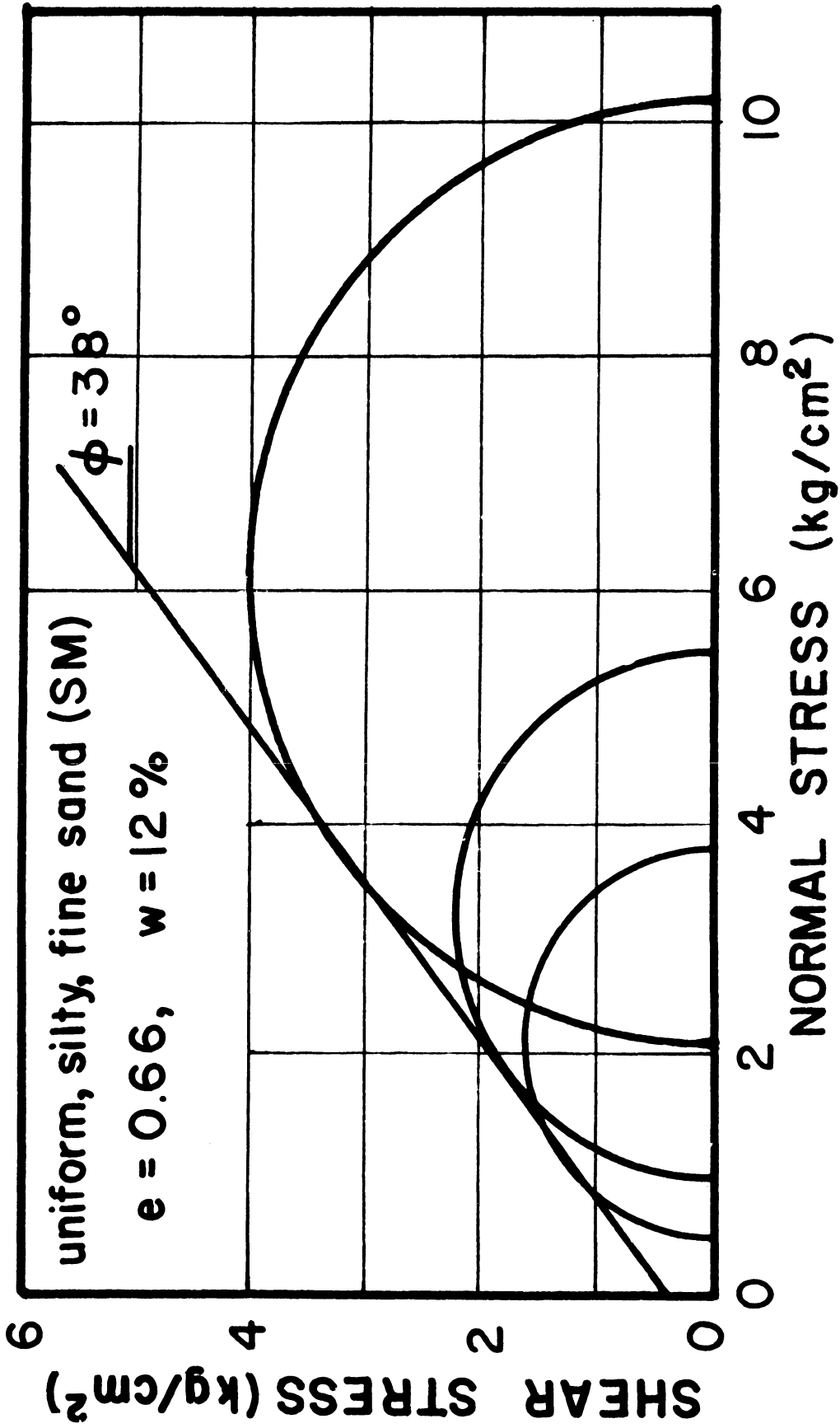


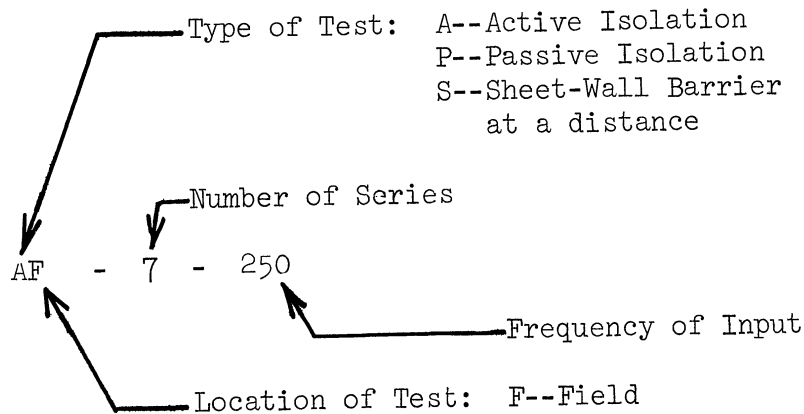
Figure 7. Mohr's Circle Diagram for Drained Triaxial Tests on Undisturbed Samples. (upper layer).

Since wave length scaling was deemed appropriate for these model tests, the wave length of the Rayleigh wave (λ_R) had to be determined at the field site. Rayleigh wave velocities, v_R , and wave lengths, λ_R , as determined in the field by the method described by Fry (1963) are given in Table I. Critical dimensions of the trenches used in all tests were normalized on λ_R for the appropriate frequency when used to compare results of two or more tests at different frequencies.

ACTIVE ISOLATION TESTS

The primary variables in the active isolation tests (isolation at the source) were H and θ , where H is the trench depth and θ is the angular length of the trench. Barrier trenches 0.5 to 2.0 feet deep composed of segments of annuli ranging from 90° to 360° were employed. Figure 8 shows a schematic diagram of the experimental setup for these tests with the critical dimensions labeled and Figure 9 is a photograph of this setup. The radius, R_0 , of the annular trenches was 0.50 and 1.00 foot. By employing trenches at these two radii and by using four exciter frequencies, it was possible to obtain trench radius to wave length ratios (R_0/λ_R) ranging from 0.222 to 0.910. A list of field tests with trench dimensions is given in Table II.

A code was established to identify each test. The code consisted of two letters describing the kind of test and where it was performed, a number representing the particular test in a series, and a number giving the frequency of input motion used in that test. The code is read as follows:



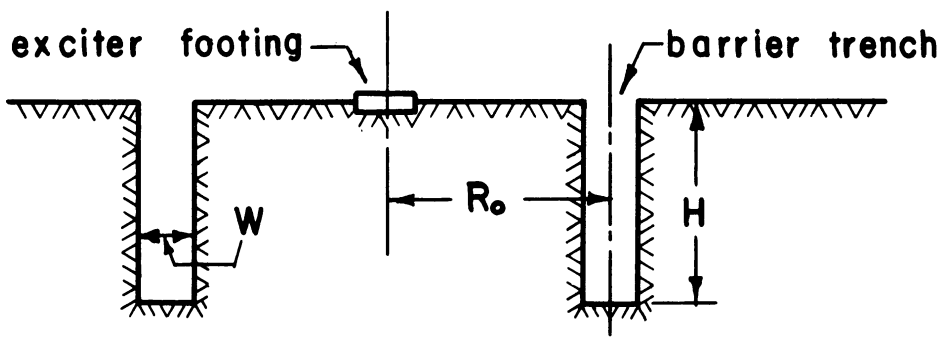
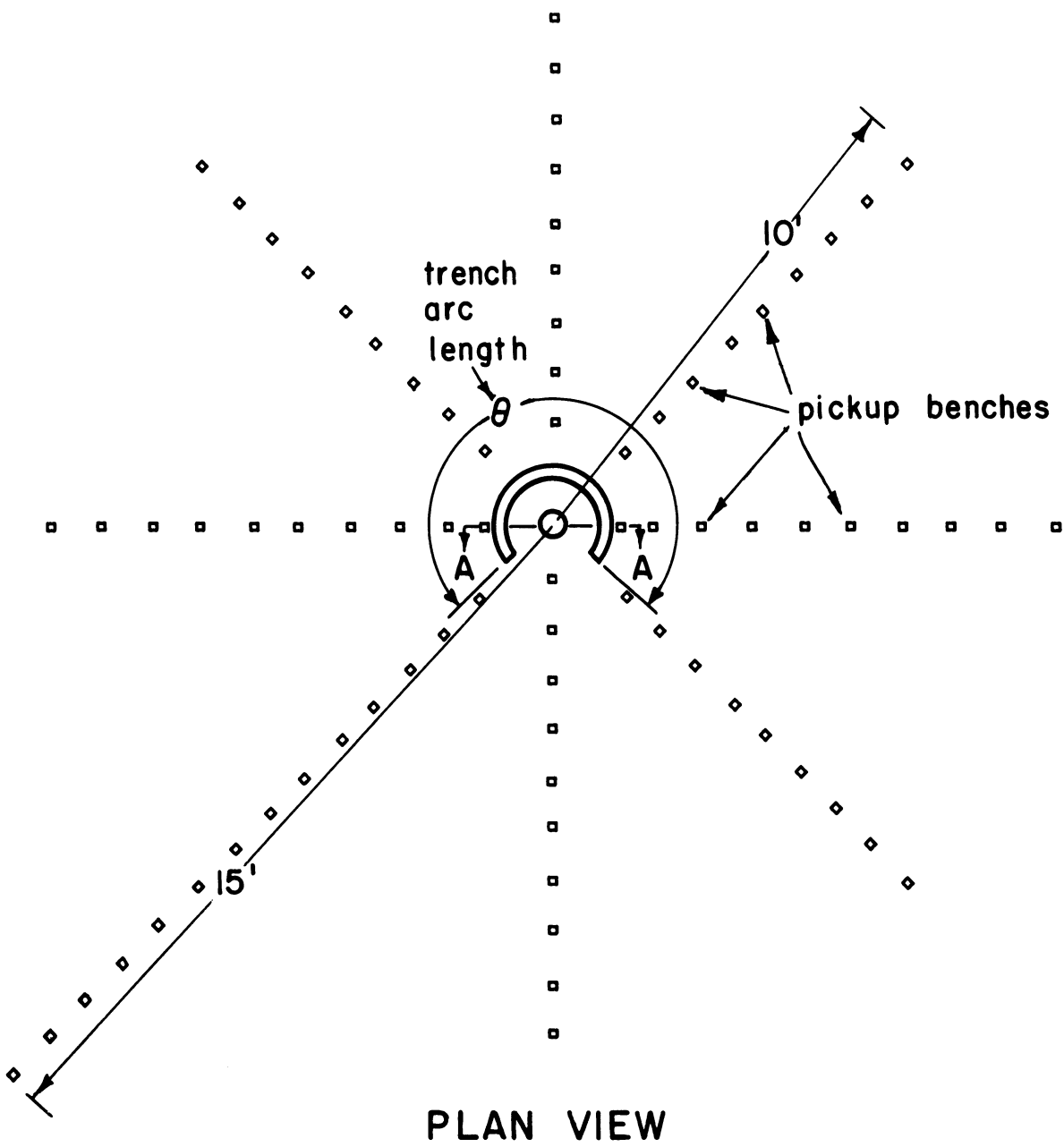


Figure 8. Schematic of Test Layout for Active Isolation in the Field.

TABLE I

WAVE LENGTH AND WAVE VELOCITY FOR THE
RAYLEIGH WAVE AT THE FIELD SITE

Frequency (cps)	λ_R (ft)	v_R (ft/sec)
200	2.25	450
250	1.68	420
300	1.38	415
350	1.10	385

TABLE II

SCHEDULE OF FIELD TESTS FOR ACTIVE ISOLATION

Test Number	Distance to Trench	Depth of Trench	Length of Trench	Frequency (cps)					
				R_0/λ_R	H/λ_R	R_0/λ_R	H/λ_R	R_0/λ_R	H/λ_R
	R_0 (ft)	H (ft)	θ (deg)	200	250	300	350	R_0/λ_R	H/λ_R
AF 1	1.0	0.5	90	0.444	0.596	0.726	0.910	0.910	0.455
AF 2	1.0	0.5	180	0.444	0.596	0.726	0.910	0.910	0.455
AF 3	1.0	1.0	180	0.444	0.596	0.726	0.910	0.910	0.910
AF 4	1.0	1.0	270	0.444	0.596	0.726	0.910	0.910	0.910
AF 5	1.0	1.0	360	0.444	0.596	0.726	0.910	0.910	0.910
AF 6	1.0	2.0	360	0.444	0.888	0.726	1.452	0.910	1.820
AF 7	1.0	0.5	360	0.444	0.222	0.726	0.363	0.910	0.455
AF 8	0.5	0.5	90	0.222	0.298	0.363	0.363	0.455	0.455
AF 9	0.5	0.5	180	0.222	0.298	0.363	0.363	0.455	0.455
AF 10	0.5	0.5	270	0.222	0.298	0.363	0.363	0.455	0.455
AF 11	0.5	0.5	360	0.222	0.298	0.363	0.363	0.455	0.455
AF 12	0.5	1.0	360	0.222	0.444	0.363	0.726	0.455	0.910

$W = 0.25$ for all trenches

$W/\lambda_R = 0.110$ $W/\lambda_R = 0.149$

$W/\lambda_R = 0.182$

$W/\lambda_R = 0.228$

For all of the active isolation tests, the effectiveness criteria were applied to the test results to determine the minimum effective trench depth. Two methods were used to select the trenches which satisfied the criteria for amplitude reduction and area of influence. In the first method an average of the amplitude reduction factors for eight radial lines was plotted versus distance from the source. For a trench to qualify as "effective", the curve of average amplitude factors had to be 0.25 or lower. Figure 10 shows an example of this selection method for three tests. Two tests, AF-5-300 and AF-6-300, satisfied the criteria, while one test, AF-7-300, did not satisfy the criteria. In the second method amplitude reduction factor contour diagrams for each test were studied to determine those tests for which at least 75 percent of the area outside the trench was reduced in amplitude by a factor of 0.25 or less. Amplitude reduction factor contour diagrams for the three tests shown on Figure 10 are given on Figures 11, 12, and 13 for comparison. (Note: 27 amplitude reduction factor contour diagrams similar to Figures 11, 12, and 13 can be found in Woods (1967)). According to the criteria, tests AF-5-300 and AF-6-300 passed again while test AF-7-300 failed. The definition of the amplitude reduction factor is repeated on Figure 11 but will not be shown on subsequent figures.

All of the full circle active isolation tests listed in Table II were evaluated using the above methods. The tests with full circle trenches at a radius of 1.00 foot are listed in order of increasing scaled depth, or increasing H/λ_R , in Table III. All of the tests above the double line did not meet the criteria for effective screening, while those below the double line did. This would suggest

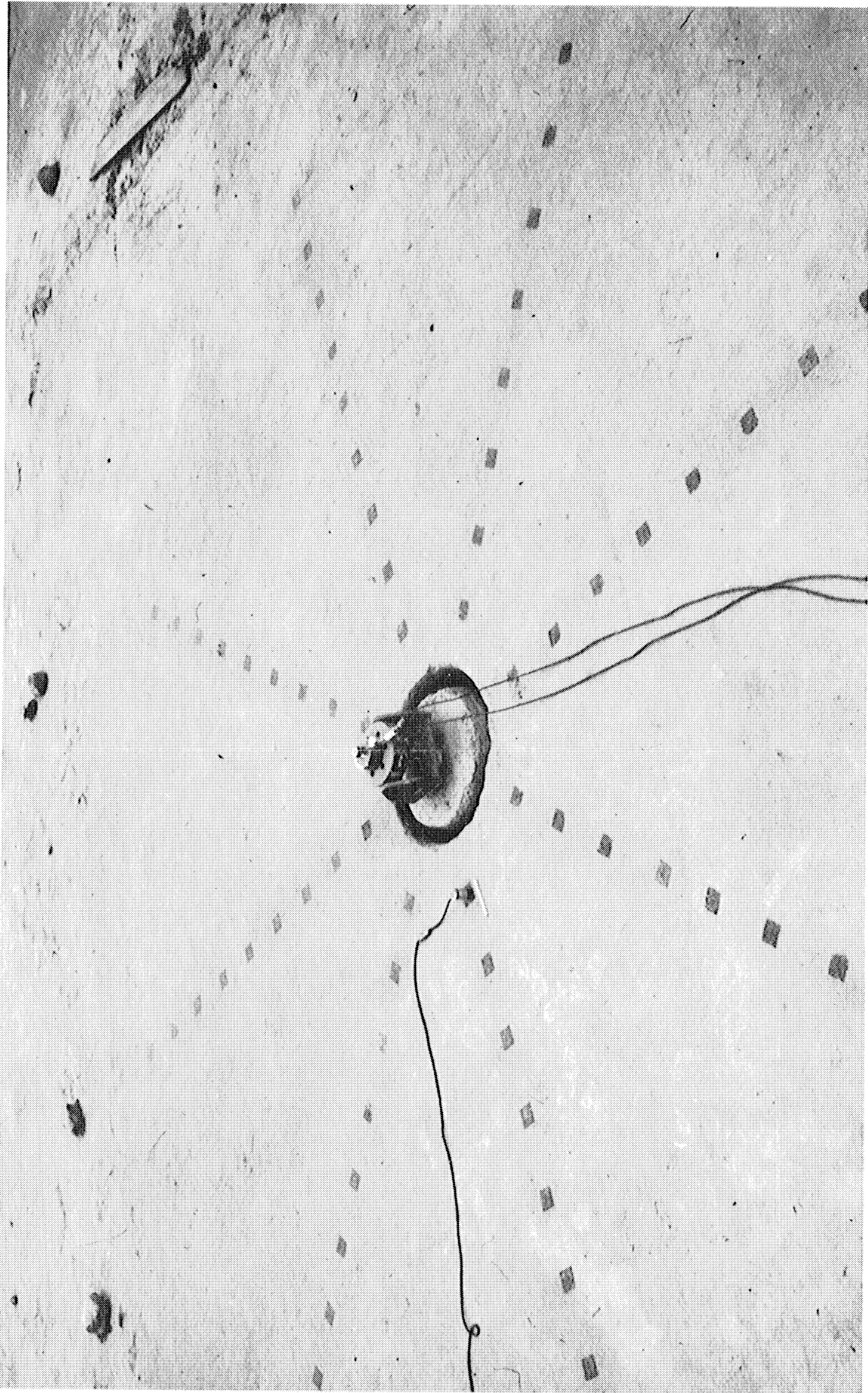


Figure 9. Photograph of Field Test Layout for Isolation at the Source.

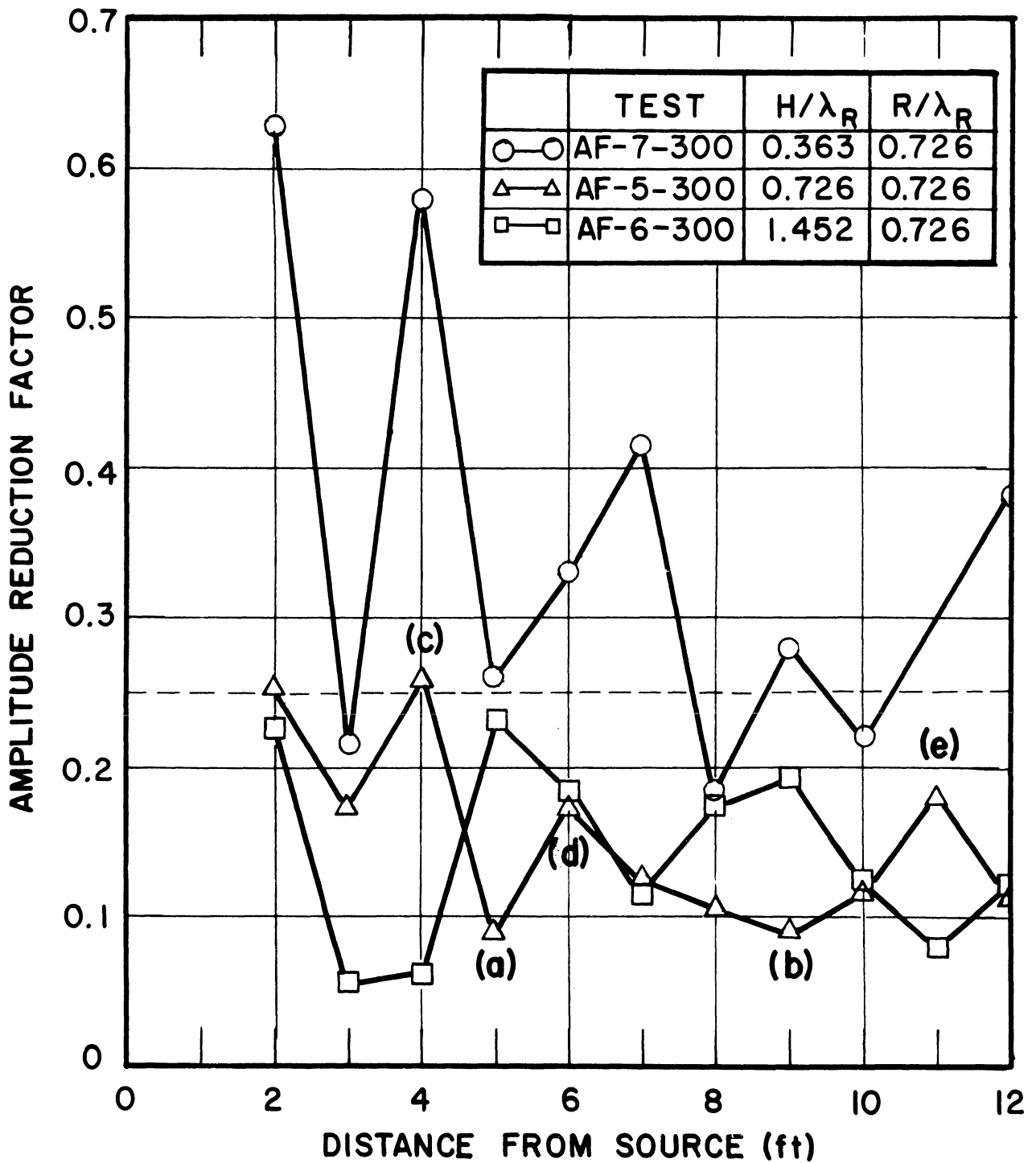
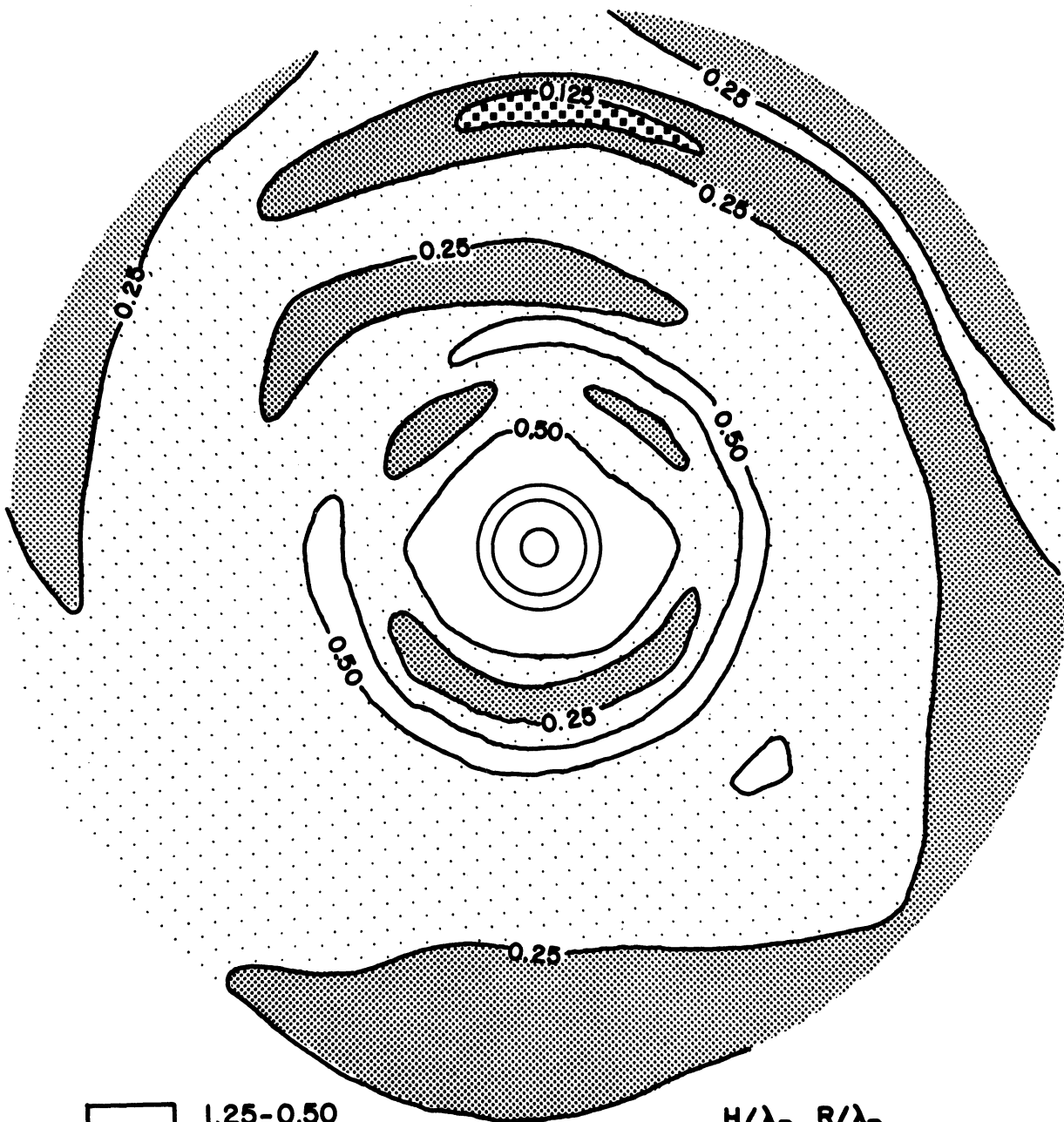

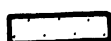




Figure 10. Amplitude Reduction Factor Versus Distance from Source-- Three Tests.



-  1.25-0.50
-  0.50-0.25
-  0.25-0.125
-  < 0.125

H/λ_R R/λ_R
0.363 0.726

AMPLITUDE REDUCTION FACTOR = $\frac{\text{Amplitude after trench}}{\text{Amplitude before trench}}$

Figure 11. Amplitude Reduction Factor Contour Diagram, Test AF-7-300.

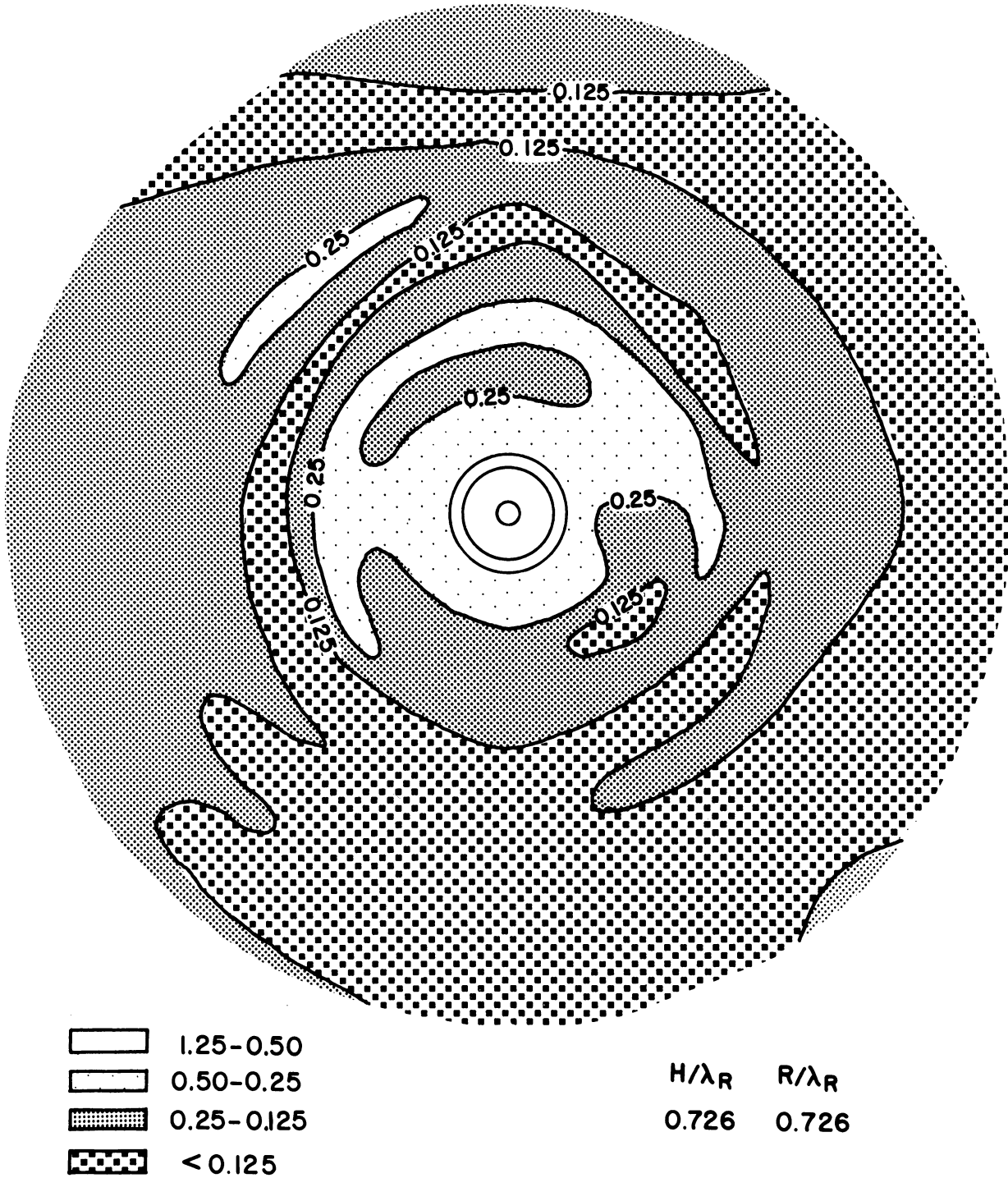
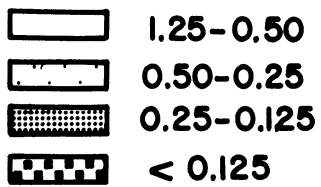
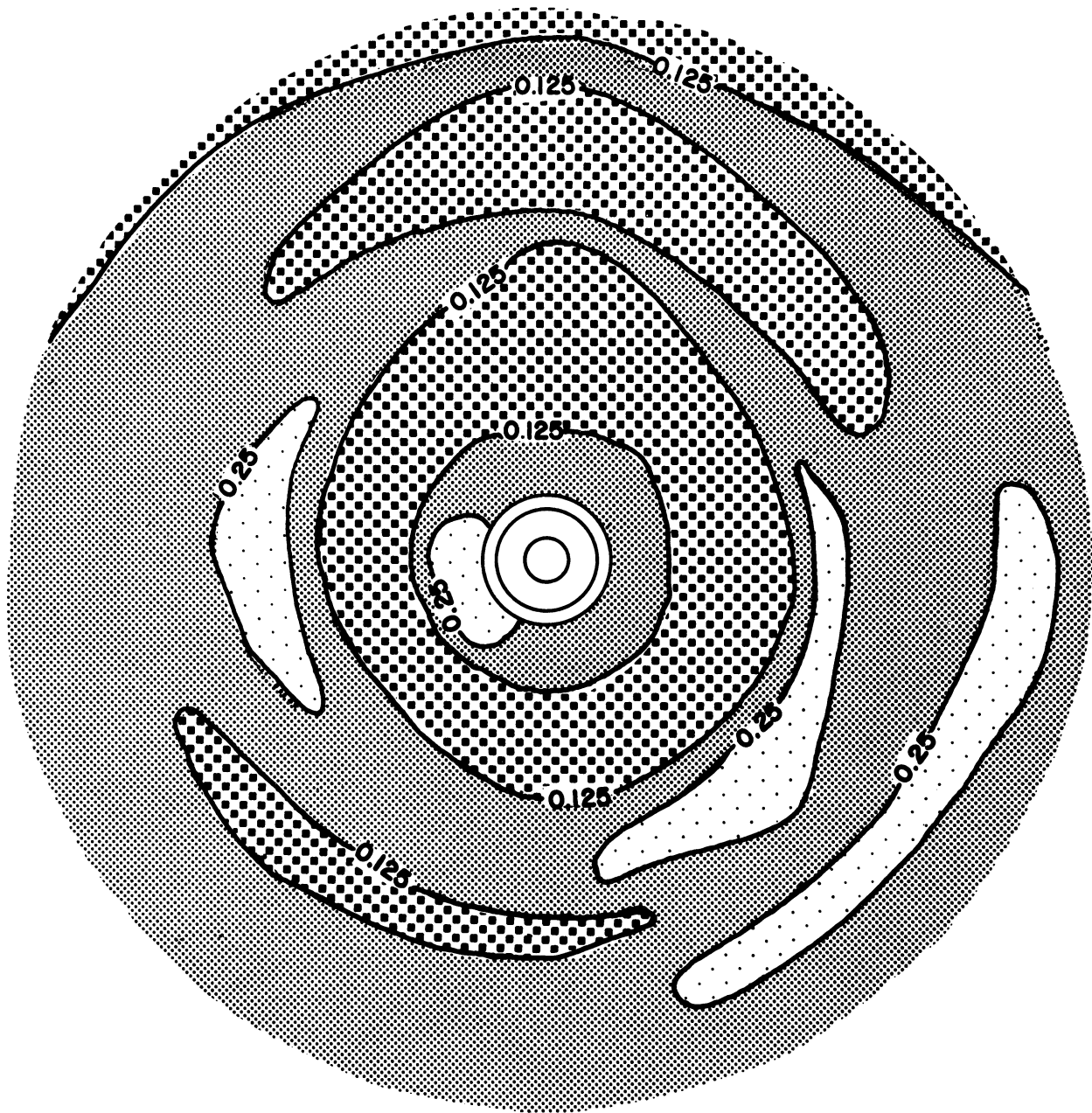


Figure 12. Amplitude Reduction Factor Contour Diagram, Test AF-5-300.



H/λ_R	R/λ_R
1.452	0.726

Figure 13. Amplitude Reduction Factor Contour Diagram, Test AF-6-300.

TABLE III

ACTIVE ISOLATION TESTS WITH TRENCH LENGTH
 θ , 360° AND TRENCH RADIUS, R_o , 1.0 FOOT

TEST NO.	H/λ_R		R_o/λ_R
AF-7-200	0.222		0.444
AF-7-250	0.298	Did Not Meet Criteria	.0596
AF-7-300	0.363		0.726
AF-5-200	0.444		0.444
AF-7-350	0.455		0.910
AF-5-250	0.596		0.596
AF-5-300	0.726		
AF-6-200	0.888	Met Criteria	0.444
AF-5-350	0.910		0.910
AF-6-250	1.192		0.596
AF-6-300	1.452		0.726
AF-6-350	1.820		0.910

that for full circle trenches located less than one wave length from the center of the source of vibration the scaled depth H/λ_R , must be greater than 0.60 for the trench to be effective.

The tests with full circle trenches at a radius of 0.5 foot are listed in order of increasing scaled depth in Table IV. Once again all of the tests below the double line qualified while those above did not. These results would suggest that for full circle trenches located less than one-half wave length from the center of the source of vibration the scaled depth, H/λ_R , must be greater than 0.44 for the trench to be effective. Further examination of the tests for isolation at the source indicated that amplitude reductions greater than one order of magnitude are not likely to be achieved using trench barriers up to two wave lengths ($H/\lambda_R = 2.0$) deep. The results of Barkan (1962) and Dolling (1965) indicated similar results.

From these test results it could be concluded that for full circle trenches surrounding the source of vibration at a distance of one wave length or less, the scaled depth of the trench must be about 0.6 for the trench to be effective. For full circle trenches the screened zone included an area of the half space outside of the trench extending to a radius of at least 10 wave lengths. Data was not obtained beyond 10 wave lengths due to the site size and the vibration exciter power capabilities.

For trenches of arc length less than 360° , the screened zone was an area symmetrical about a radius from the source of excitation through the center of the trench and was bounded laterally by two radial lines extending from the center of the source of excitation through

TABLE IV

ACTIVE ISOLATION TESTS WITH TRENCH LENGTH
 θ , 360° AND TRENCH RADIUS, R_o , 0.5 FOOT

TEST NO.	H/λ_R		R_o/λ_R
AF-11-200	0.222	Did Not Meet Criteria	0.222
AF-11-250	0.298		0.298
AF-11-300	0.363		0.363
AF-12-200	0.444		0.222
AF-11-350	0.455	Met Criteria	0.455
AF-12-250	0.596		0.298
AF-12-300	0.726		0.363
AF-12-350	0.910		0.455

points 45° from each end of the trench. Within this zone 75 percent of the area had to be reduced in amplitude by 0.25 for a partial circle trench to be considered effective. This definition of the screened zone excludes trenches of arc length less than 90° , and all data from these tests confirms that 90° trenches are not effective. Examples of the screened zone for two trenches of less than 360° arc length are shown on Figures 14 and 15. In these tests, also, the screened zone extended at least 10 wave lengths from the source. The same criteria for screening effectiveness (amplitude reduction of 0.25 or less) when applied to trenches of arc length less than 360° showed that the same scaled trench depth, $H/\lambda_R = 0.6$), is required to produce an effectively screened zone.

Another phenomenon noted in the active isolation tests with 360° trenches was that the amplitude reduction factor undergo a series of relative maxima and minima with increasing distance from the barrier. This is demonstrated by the curves of amplitude of vertical displacement versus distance from the source on Figure 10 where points marked (a) and (b) on the curve for test AF-5-300 are points of relative minima and points (c), (d), and (e) are points of relative maxima. This phenomenon can also be seen in the amplitude reduction factor contour diagram shown in Figure 13.

Although there were several relative maxima and minima for each test, there was usually only one "principal minimum." The location of this "principal minimum" was investigated to determine whether it consistently occurred in the same location. Four curves of amplitude reduction factor versus distance from the source (in wave lengths) from

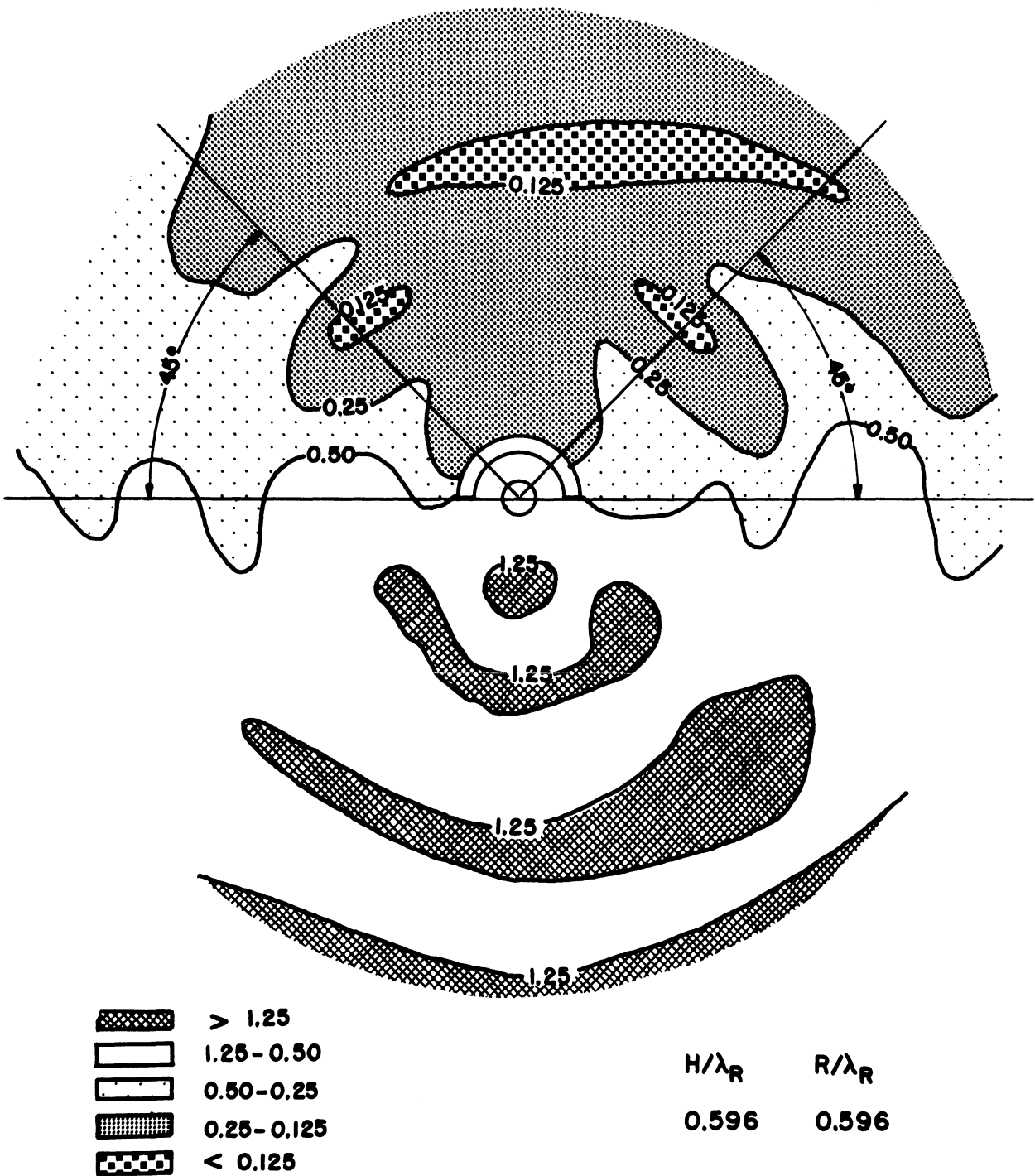
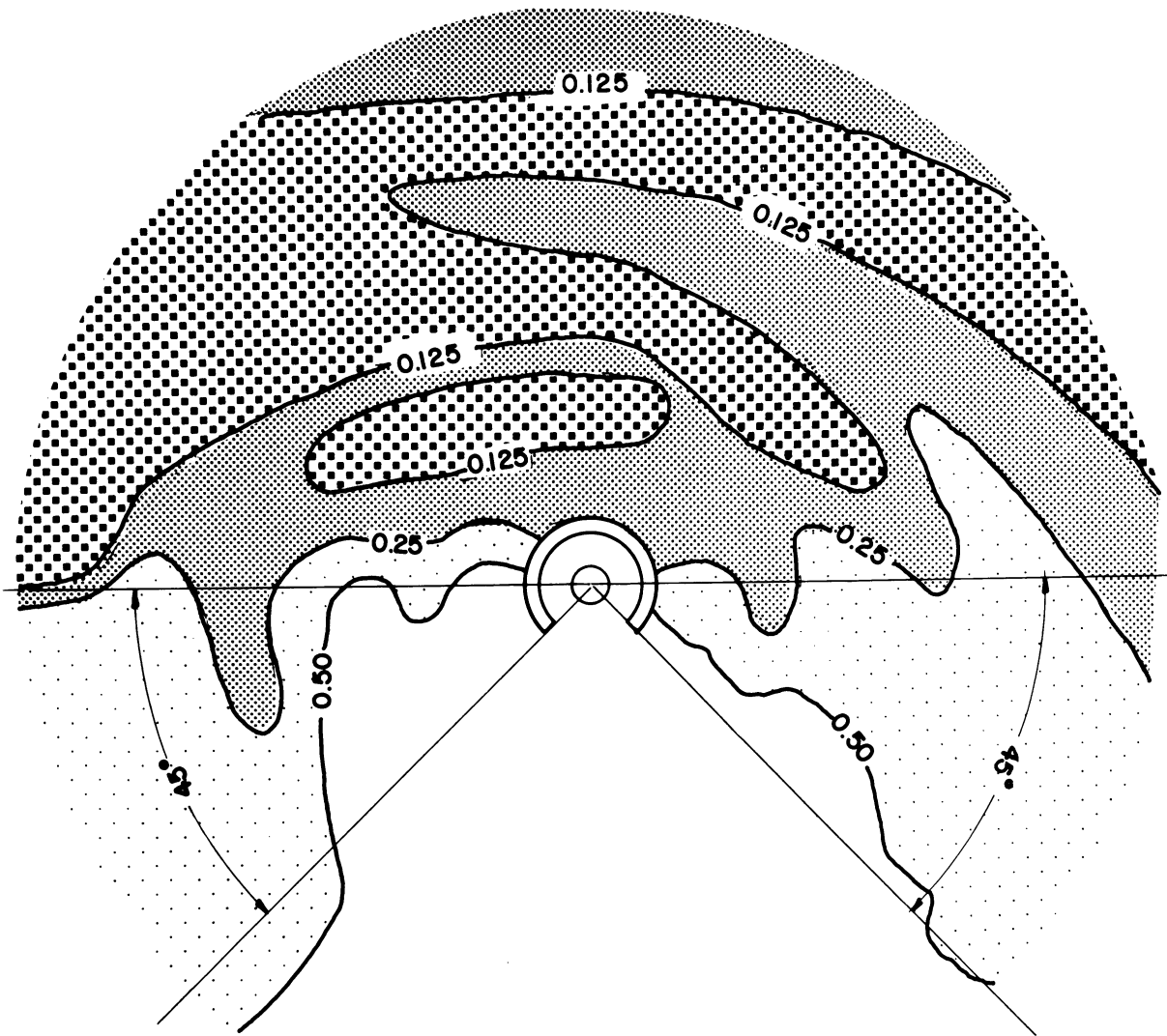


Figure 14. Amplitude Reduction Factor Contour Diagram, Test AF-3-250.



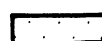
	1.25-0.50	H/λ_R	R/λ_R
	0.50-0.25	0.726	0.726
	0.25-0.125		
	<0.125		

Figure 15. Amplitude Reduction Factor Contour Diagram, Test AF-4-300.

typical tests with full circle trenches, 1.0 foot deep, are shown in Figure 16. For the four tests shown the "principal minimum" occurred at about the same number of wave lengths from the source of excitation, 3.5 to 4.0 wave lengths. Similar curves for all full circle tests at a 1.0 foot radius were examined, and the location of the "principal minimum," in wave lengths from the source, is shown in Table V. The indications of the results presented in Table V were that the distance from the source to the "principal minimum" decreases as the depth of the trench increases.

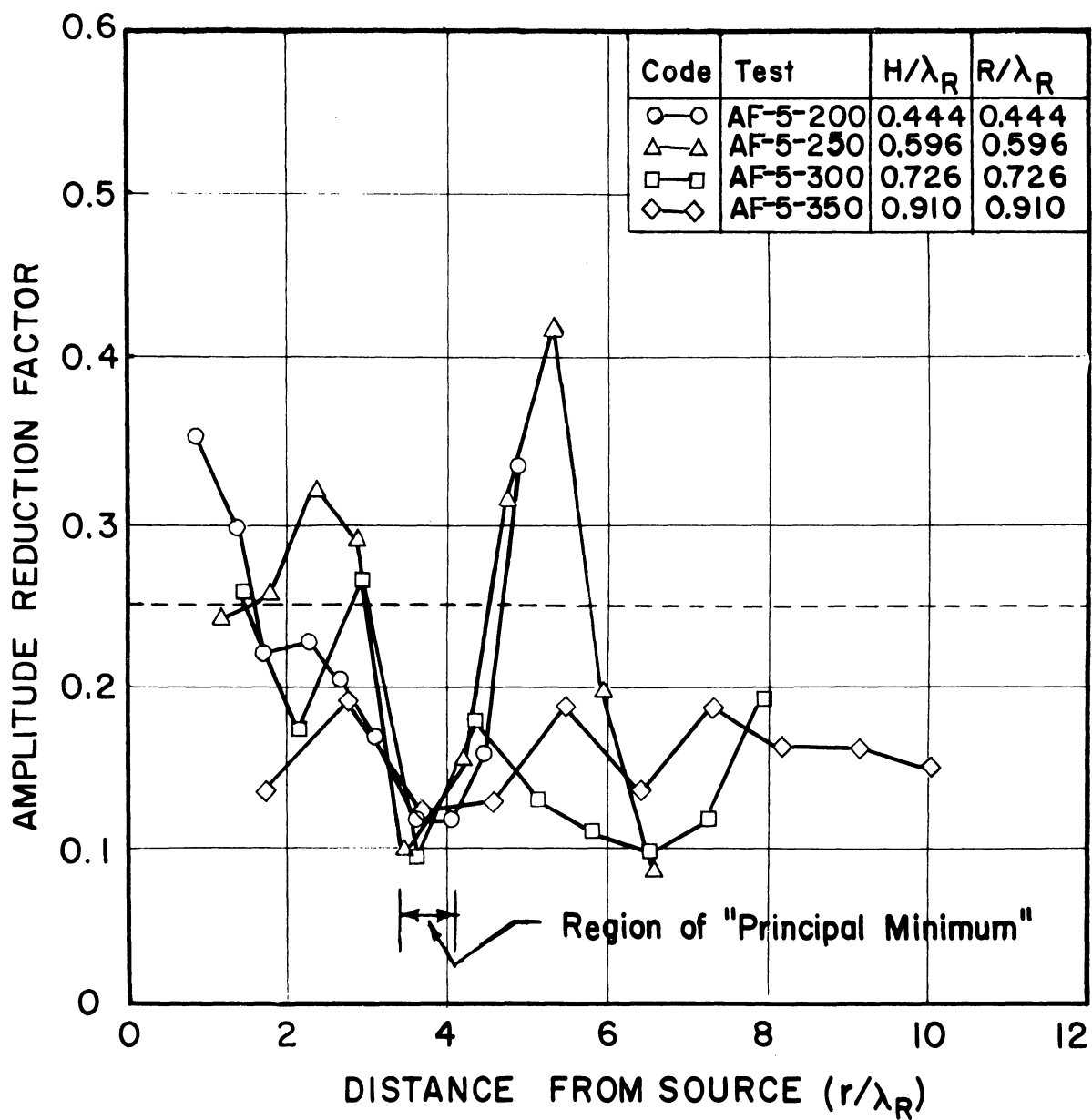


Figure 16. Amplitude Reduction Factor Versus Distance from Source-- Location of "Principal Minimum."

TABLE V

DISTANCE FROM THE SOURCE OF VIBRATION TO THE
"PRINCIPAL MINIMUM" (IN WAVE LENGTHS) FOR FULL
CIRCLE ACTIVE ISOLATION TESTS

Frequency of Vibration (cps)	Depth of Trench (ft)		
	0.5	1.0	2.0
200	4.0	3.5	3.1
250	2.4	3.6	3.6
300	5.8	3.6	2.2
350	6.4	3.6	2.7

PASSIVE ISOLATION TESTS

One test setup for passive isolation is shown in the overall field site photo on Figure 4. This same test layout is shown schematically on Figure 17. The layout consisted of two vibration exciter footings, a trench barrier, and 75 pickup benches. For this series of tests it was assumed that the zone screened by the trench would be symmetrical about the 0° line; therefore surface motion measurements were made for only one-half of the screened zone. Symmetry of screening effects had been already sufficiently established in the active isolation tests. The variables in these tests were trench depth, H , trench length, L , trench width, W , and distance from the source of excitation to the trench, R .

To study passive isolation, trenches ranging in size from 1.0 foot deep by 1.0 foot long by 0.33 foot wide, to 4.0 feet deep by 8.0 feet long by 1.0 foot wide were employed. By locating the vibration exciter at two distances from these trenches and using four frequencies of excitation, 200, 250, 300, and 350 cps, a range of eight R/λ_R ratios ($R/\lambda_R = 2.22$ to 9.10) was obtained. This range in R/λ_R was necessary to evaluate the effects of the exciter-trench distance, R , on trench performance. A list showing the dimensions of the trenches used in this series is given in Table VI.

Amplitude reduction and area of influence criteria were applied to the results of the tests for trenches at each distance from the source. To satisfy the area criterion a semicircular zone behind the trench with center at the midlength of the trench and radius of

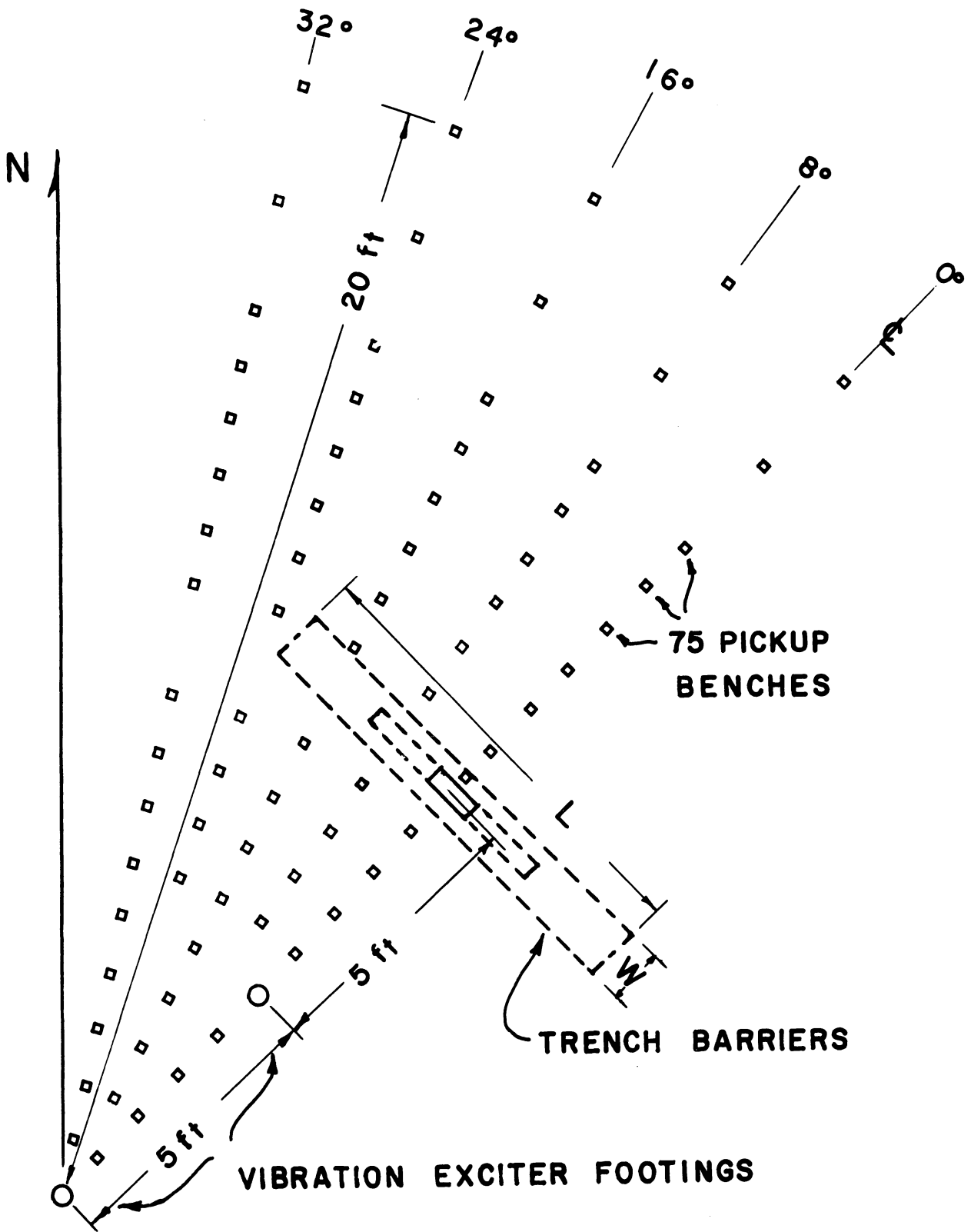


Figure 17. Plan View of Field Site Layout for Screening at a Distance.

TABLE VI
SCHEDULE OF FIELD TESTS FOR PASSIVE ISOLATION

Test Number	Dist. to Trench R (ft)	Depth of Trench H (ft)	Length of Trench L (ft)	Frequency (cps)											
				200			250			300			350		
				R/λ_R	L/λ_R	W/λ_R	R/λ_R	L/λ_R	W/λ_R	R/λ_R	L/λ_R	W/λ_R	R/λ_R	L/λ_R	W/λ_R
PF 1	10	1.0	1.0	0.44	0.44	0.13	0.59	0.59	0.17	0.73	0.73	0.21	0.91	0.91	0.26
PF 3	10	1.0	2.0	0.44	0.89	0.13	0.59	0.19	0.17	0.73	1.46	0.21	0.91	1.82	0.26
PF 5	10	1.0	3.0	0.44	1.33	0.13	0.59	1.79	0.17	0.73	2.18	0.21	0.91	2.73	0.26
PF 7	10	2.0	3.0	0.89	1.33	0.13	1.19	1.79	0.17	1.46	2.18	0.21	1.82	2.73	0.26
PF 9	10	2.0	4.0	0.89	1.78	0.13	1.19	2.38	0.17	1.46	2.90	0.21	1.82	3.64	0.26
PF 11	10	2.0	6.0	0.89	2.66	0.13	1.19	3.57	0.17	1.46	4.35	0.21	1.82	5.47	0.26
PF 13	10	3.0	6.0	1.33	2.66	0.13	1.79	3.57	0.17	2.18	4.35	0.21	2.73	5.47	0.26
PF 15	10	3.0	8.0	1.33	3.55	0.13	1.79	4.76	0.17	2.18	5.80	0.21	2.73	7.29	0.26
PF 17	10	4.0	8.0	1.78	3.55	0.13	2.38	4.76	0.17	2.90	5.80	0.21	3.64	7.29	0.26
PF 19	10	2.0*	8.0	0.89	3.55	0.13	1.19	4.76	0.17	1.46	5.80	0.21	1.82	7.29	0.26
PF 21	10	4.0	8.0	1.78	3.55	0.44	2.38	4.76	0.59	2.90	5.80	0.73	3.64	7.29	0.91
PF 23	10	2.0*	8.0	0.89	3.55	0.44	1.19	4.76	0.59	1.46	5.80	0.73	1.82	7.29	0.91
				$R/\lambda_R = 2.22$			$R/\lambda_R = 2.98$			$R/\lambda_R = 3.62$			$R/\lambda_R = 4.55$		
PF 2	5	1.0	1.0	0.44	0.44	0.13	0.59	0.59	0.17	0.73	0.73	0.21	0.91	0.91	0.26
PF 4	5	1.0	2.0	0.44	0.89	0.13	0.59	1.19	0.17	0.73	1.46	0.21	0.91	1.82	0.26
PF 6	5	1.0	3.0	0.44	1.33	0.13	0.59	1.79	0.17	0.73	2.18	0.21	0.91	2.73	0.26
PF 8	5	2.0	3.0	0.89	1.33	0.13	1.19	1.79	0.17	1.46	2.18	0.21	1.82	2.73	0.26
PF 10	5	2.0	4.0	0.89	1.78	0.13	1.19	2.38	0.17	1.46	2.90	0.21	1.82	3.64	0.26
PF 12	5	2.0	6.0	0.89	2.66	0.13	1.19	3.57	0.17	1.46	4.35	0.21	1.82	5.47	0.26
PF 14	5	3.0	6.0	1.33	2.66	0.13	1.79	3.57	0.17	2.18	4.35	0.21	2.73	5.47	0.26
PF 16	5	3.0	8.0	1.33	3.55	0.13	1.79	4.76	0.17	2.18	5.80	0.21	2.73	7.29	0.26
PF 18	5	4.0	8.0	1.78	3.55	0.13	2.38	4.76	0.17	2.90	5.80	0.21	3.64	7.29	0.26
PF 20	5	2.0*	8.0	0.89	3.55	0.13	1.19	4.76	0.17	1.46	5.80	0.21	1.82	7.29	0.26
PF 22	5	4.0	8.0	1.78	3.55	0.44	2.38	4.76	0.59	2.90	5.80	0.73	3.64	7.29	0.91
PF 24	5	2.0	8.0	0.89	3.55	0.44	1.19	4.76	0.59	1.46	5.80	0.73	3.64	7.29	0.91

* Backfilled from 4.0 feet

one-half trench length had to be reduced in amplitude by 0.25 or less. From practical considerations the critical dimension for trench barriers was the scaled depth, H/λ_R , therefore for each distance from the source the shallowest trench which satisfied the criteria was determined. The shallowest effective trenches are listed in order of increasing scaled distance, R/λ_R , in Table VII and are underlined in Table VI. Of the 96 tests in this series for passive isolation, 35 satisfied the criteria. The minimum scaled depth for the full range of R/λ_R was generally between $H/\lambda_R = 1.2$ and $H/\lambda_R = 1.5$. To evaluate the effect of total trench area on the screened zone, a quantity HL/λ_R^2 (scaled trench length times scaled trench depth) was computed for each trench. This quantity is listed in the last column of Table VII. There was a general trend toward increasing HL/λ_R^2 with increasing R/λ_R . Figure 18 shows the amplitude reduction factor contour diagram for test PF-12-250, the shallowest trench at R/λ_R equal 2.97 to satisfy the criteria.

Amplitude magnification (indicated by amplitude reduction factor contours greater than 1.0) can be seen on Figure 18 in front of and near the end of the trench. This phenomenon may explain some of the earlier unsatisfactory applications of trench barriers referred to by Barkan (1962).

Curves of amplitude of vertical displacement versus distance from the vibrator for five tests are shown in Figure 19. The increasing effectiveness of the larger trenches can be seen in the region behind the trench by the relative position of the curves for each test. Also in this figure the magnification in front of the trench and maximum reduction at some distance behind the trench are apparent.

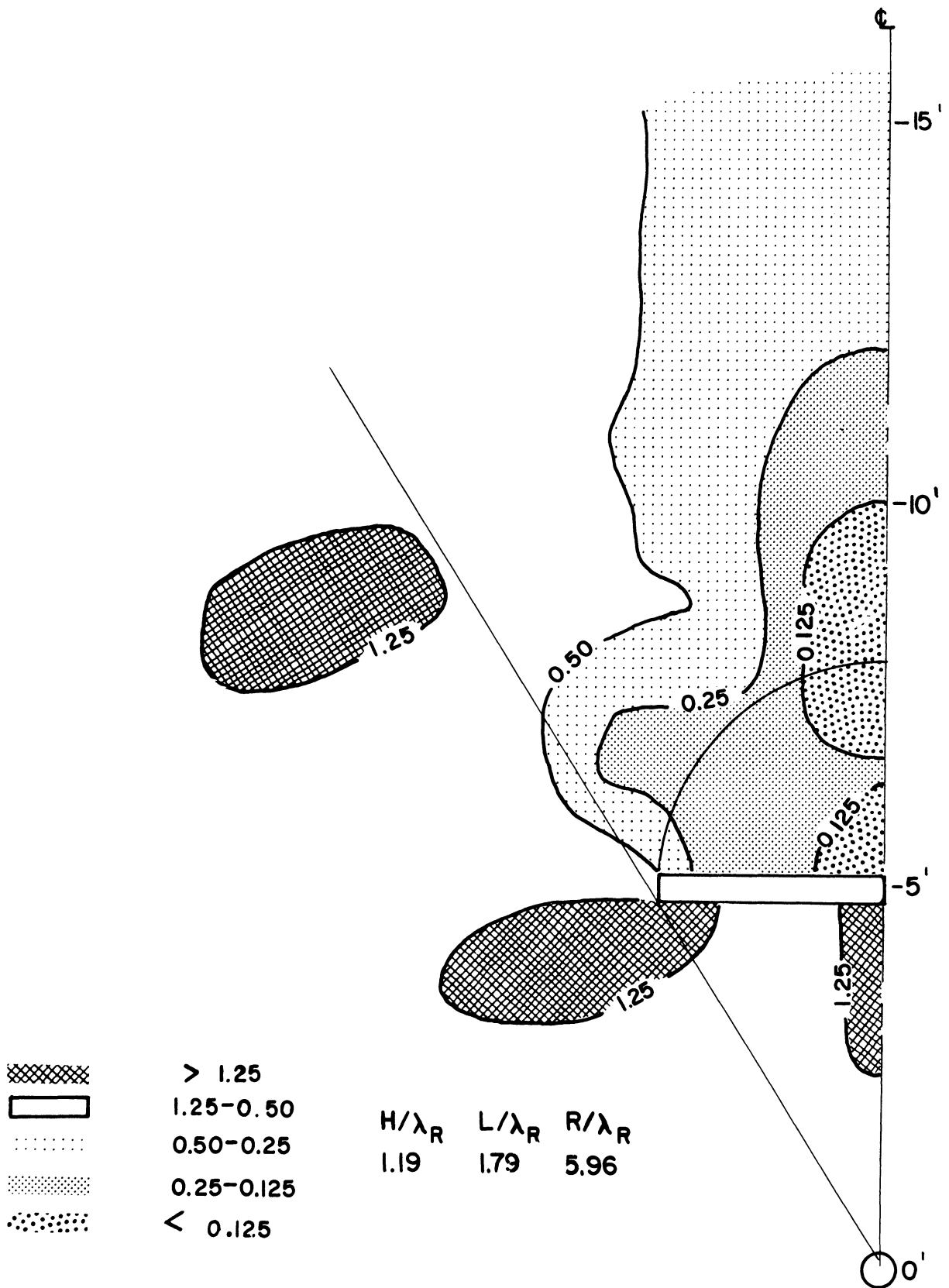


Figure 18. Amplitude Reduction Factor Contour Diagram, Test PF-12-250.

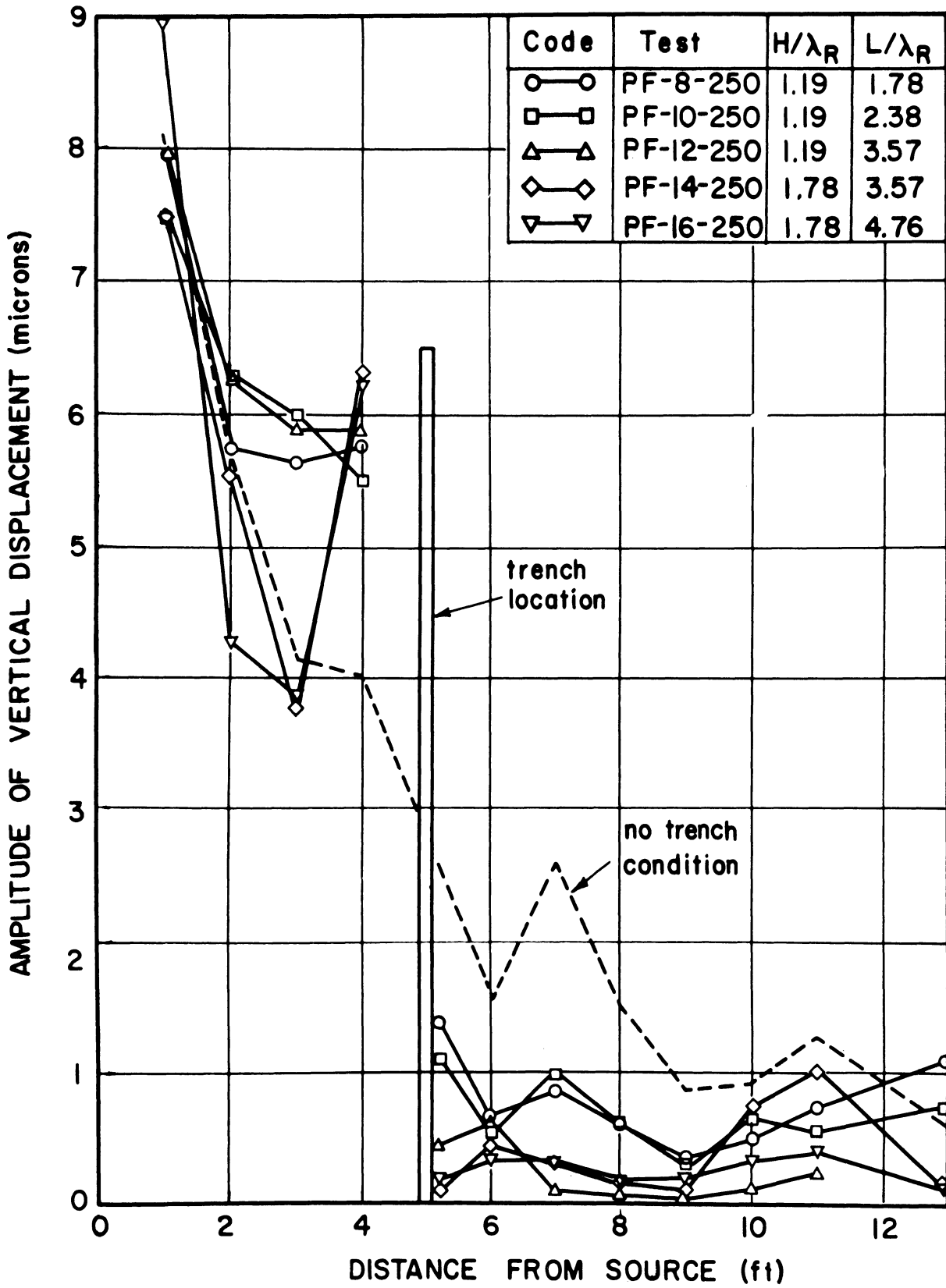


Figure 19. Amplitude of Vertical Displacement Versus Distance from Source for Five Tests.

TABLE VII
SHALLOWEST TRENCHES WHICH SATISFIED SCREENING CRITERIA
IN PASSIVE ISOLATION TESTS

TEST NO.	R/λ_R	H/λ_R	L/λ_R	HL/λ_R^2
PF-14-200	2.22	1.33	2.66	3.54
PF-12-250	2.97	1.19	3.57	4.25
PF-10-300	3.62	1.45	2.90	4.20
PF-15-200	4.44	1.35	3.55	4.73
PF-10-350	4.55	1.82	3.64	6.62
PF-11-250	5.95	1.19	3.57	4.25
PF-11-300	7.25	1.45	4.35	6.30

In planning the tests it was assumed that the width of an open trench would not be an important variable and that, in fact, a small crack or slit would be sufficient to screen elastic waves. A few tests were performed to evaluate this assumption. A comparison of the amplitude reduction factor contour diagram of test PF-17-250 shown on Figure 20 for a trench 0.33 foot wide with that of test PF-21-250 on Figure 21 for a trench 1.0 foot wide indicated that the increased width of a trench did not cause a significant change in either the magnitude of reduction or the shape of the screened zone. These results tend to confirm the assumption that trench width is not an important variable.

Another assumption made in planning this research program was that open trenches would be more effective than sheet-walls as surface wave barriers, but to satisfy the questions of many observers, a few sheet-wall barrier tests were performed. For the sheet-wall tests listed in Table VIII, an aluminum sheet $3/16$ inches thick, 4 feet deep, and 8 feet long was used as the barrier. For comparison the length and depth of the sheet-wall barrier for test SF-6-250 shown on Figure 22 were the same as the length and depth of the trench barrier for test PF-17-250 shown on Figure 20. In general the sheet-wall barriers were not as effective in reducing amplitude of vertical ground displacement as the trench barriers.

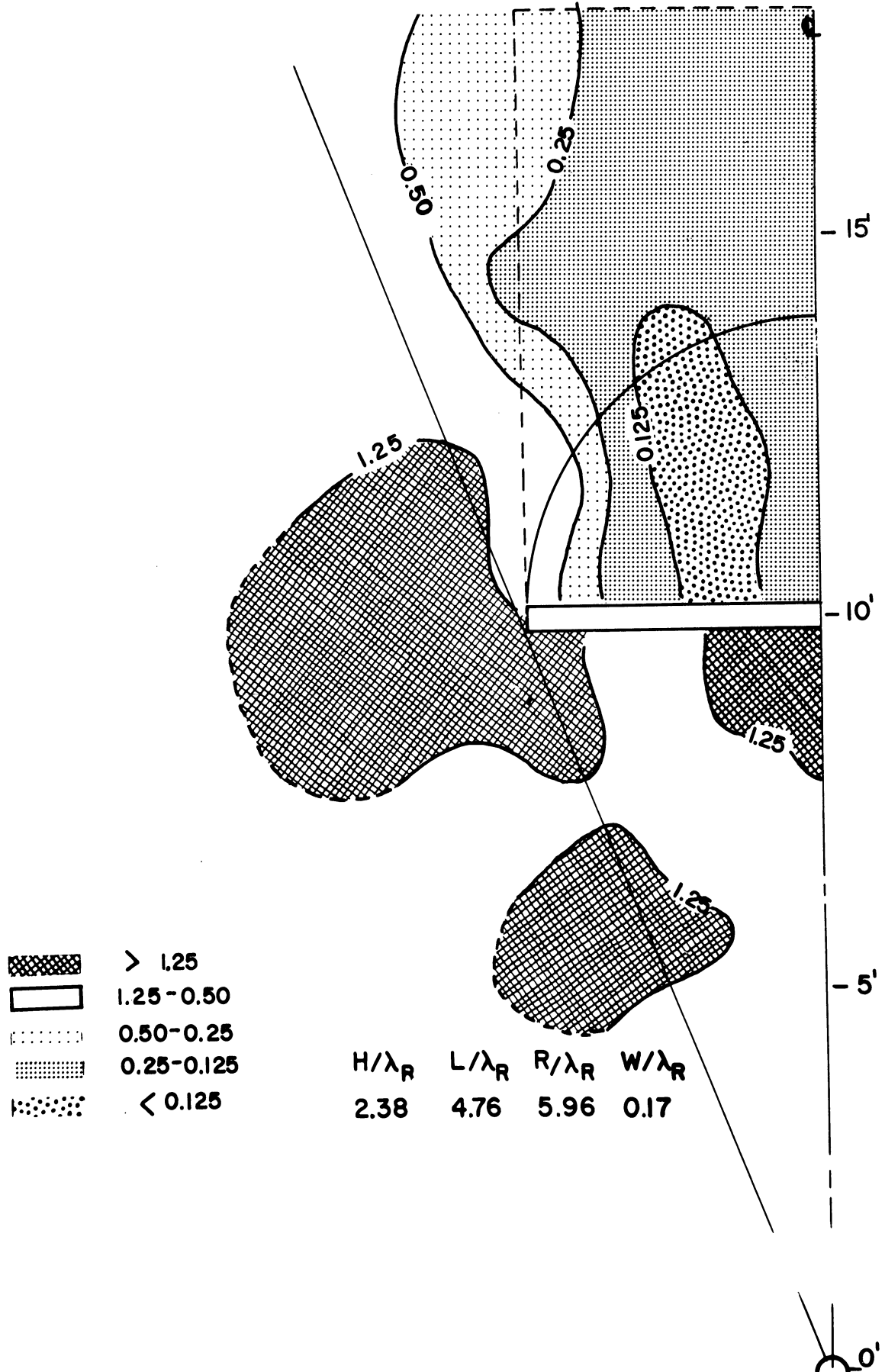


Figure 20. Amplitude Reduction Factor Contour Diagram, Test PF-17-250.

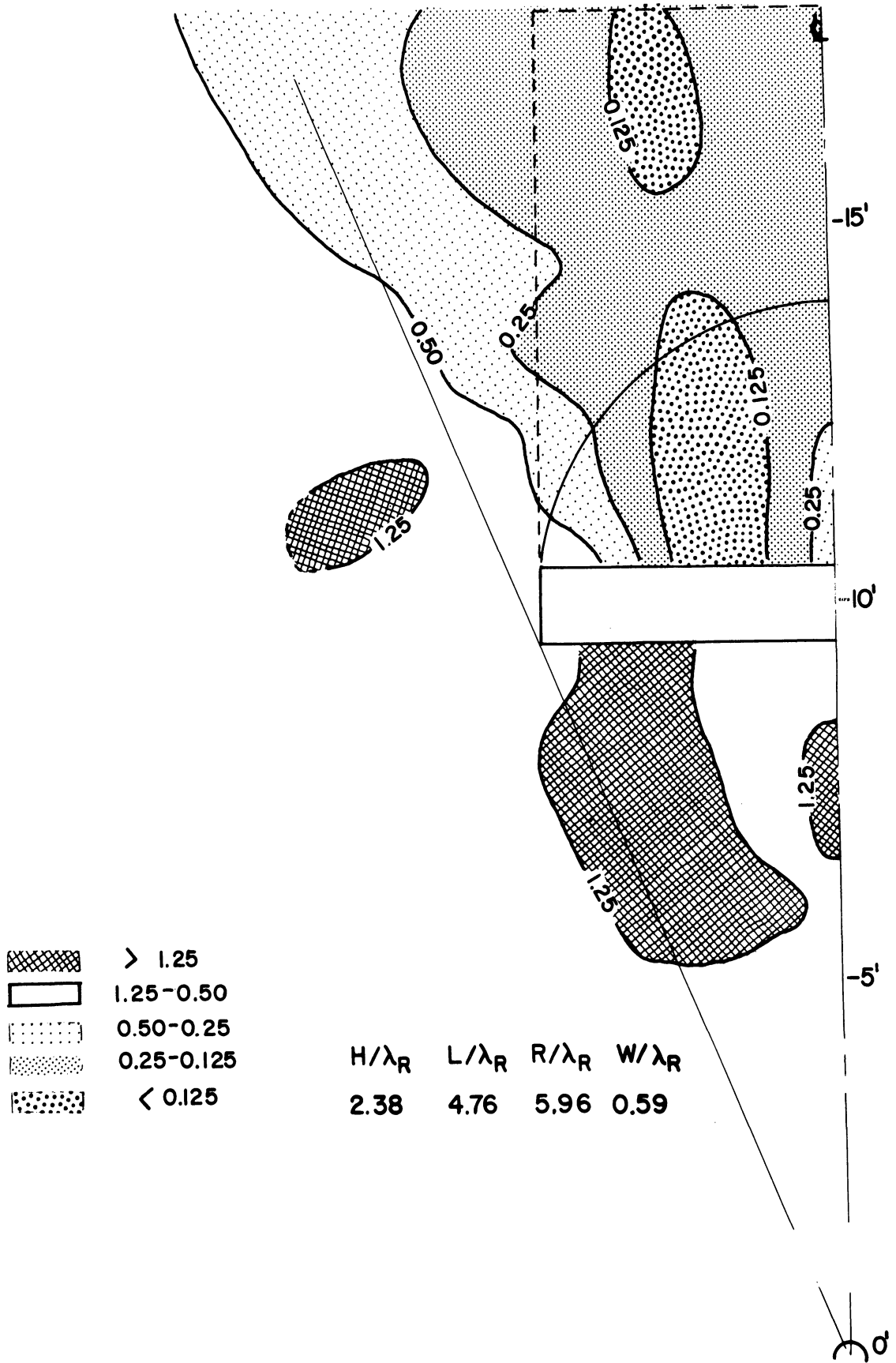


Figure 21. Amplitude Reduction Factor Contour Diagram, Test PF-21-250.

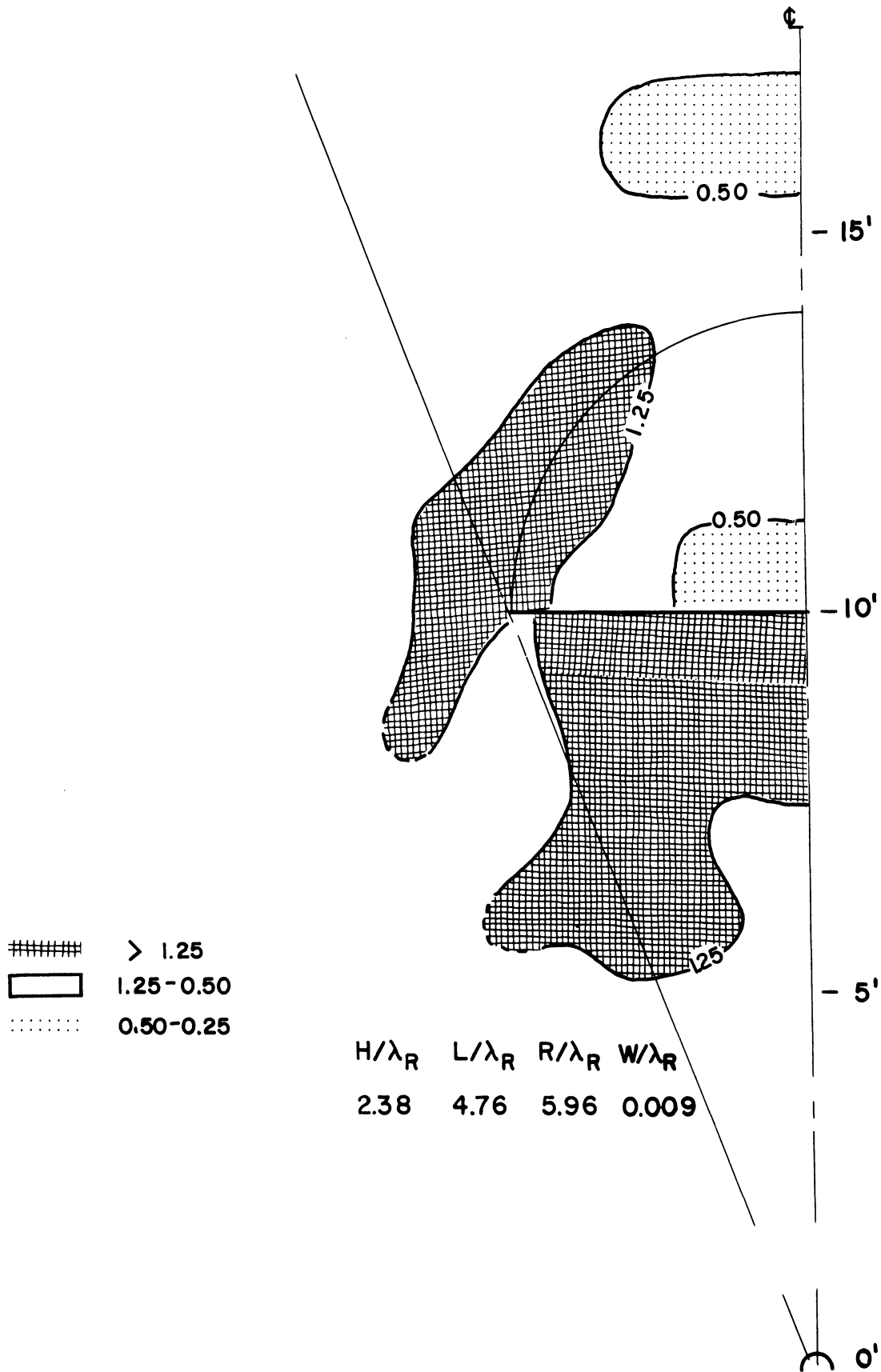


Figure 22. Amplitude Reduction Factor Contour Diagram, Test SF-6-250.

TABLE VIII

LIST OF TESTS USING SHEET-WALL BARRIERS

TEST NO.	R/λ_R	H/λ_R	L/λ_R	W/λ_R
SF-1-200	2.22	1.77	3.55	0.007
SF-2-250	2.97	2.38	4.76	0.009
SF-3-300	3.62	2.90	5.80	0.011
SF-4-350	4.55	3.64	7.29	0.014
SF-5-200	4.44	1.77	3.55	0.007
SF-6-250	5.95	2.38	4.76	0.009
SF-7-300	7.24	2.90	5.80	0.011
SF-8-350	9.10	3.64	7.28	0.014

CONCLUSIONS

Field tests were conducted to evaluate the effectiveness of open trenches in reducing the amplitude of vertical ground motion. Annular trenches surrounding the source of vibration were used in tests designated as Active Isolation. Straight trenches were used at a distance from the source but near an area to be shielded in tests designated as Passive Isolation. The parameters varied in the active isolation tests were: distance from the source to the centerline of the trench, R_0 ; depth of trench, H ; and angular length of the trench, θ . The parameters varied in the passive isolation tests were: distance from the source to the centerline of the trench, R ; depth of the trench, H ; length of the trench L ; and width of the trench, W .

To compare various tests the geometrical parameters were expressed in a dimensionless form by relating them to the wave length of the Rayleigh wave.

Conclusions from Active Isolation Tests

For full circle trenches at R/λ_R distances from 0.222 to 0.910 and for H/λ_R depths between 0.222 and 1.82, the following conclusions were made:

- (1) A minimum depth of $H/\lambda_R = 0.6$ was required for a trench to satisfy the amplitude reduction criterion of 0.25,
- (2) The zone screened by a full circle trench ($\theta = 360^\circ$) extended to a distance of at least 10 wave lengths ($10\lambda_R$) from the source of excitation,

- (3) Within the screened zone there was a specific distance from the source at which a "principal minimum" in amplitude reduction factor occurred and in these tests the "principal minimum" occurred at $2.2\lambda_R$ to $6.4\lambda_R$ from the source,
- (4) The distance from the source to the "principal minimum" decreased with increasing trench depth.

For partial circle trenches at distance R/λ_R from 0.222 to 0.910 and for depths H/λ_R between 0.222 and 1.82, the following conclusions were made:

- (1) A minimum depth of $H/\lambda_R = 0.6$ was required for a trench to provide a screened zone with an amplitude reduction factor of 0.25,
- (2) The zone screened by a partial circle trench was defined as the area outside the trench, extending to at least 10 wave lengths ($10\lambda_R$) from the source, and was bounded on the sides by radial lines from the center of the source through points 45° from the ends of the trench,
- (3) Partial circle trenches of angular length, θ , less than 90° did not provide an effectively screened zone,
- (4) Amplification or "focusing" of vibratory energy occurred in the direction of the open side of the trench.

Conclusions from Passive Isolation Tests

From field model tests using straight open trenches ($R/\lambda_R = 2.22$ to 9.10 and $H/\lambda_R = 0.444$ to 3.64) the following conclusions were reached:

- (1) Generally, larger trenches were required at greater distances from the source to accomplish a given amplitude reduction,
- (2) Energy focusing or magnification of vertical motion occurred in zones in front of trenches and to the side of trenches,
- (3) Sheet-wall barriers were not as effective as open trenches in screening surface waves,
- (4) Trench width had little influence on the effectiveness of open trenches for W/λ_R between 0.13 to 0.91.

APPENDIX I

REFERENCES

- Barkan, D. D. (1962). Dynamics of Bases and Foundations. McGraw-Hill, New York.
- Baron, M. L. and A. T. Matthews (1961). "Diffraction of a Pressure Wave by a Cylindrical Cavity in an Elastic Medium." Journal of Applied Mechanics. Vol. 28, Trans. ASME, Vol. 83, Series E, pp. 347-354.
- deBremaecker, J. C. (1958). "Transmission and Reflection of Rayleigh Waves at Corners." Geophysics, Vol. 23, pp. 253-266.
- Dolling, H. J. (1965). "Schwingungsisolierung von Bauwerken durch tiefe, auf geeignete Weise stabilisierte Schlitze." (Vibration Isolation of Buildings by Deep, Suitably Stabilized Slits). Sonderdruck aus VDI-Berichte 88, S. 3741.
- Ewing, W. M., W. S. Jardetzky and F. Press (1957). Elastic Waves in Layered Media. McGraw-Hill.
- Fry, Z. B. (1963). "A Procedure for Determining Elastic Modulus of Soils by Field Vibratory Techniques." U.S. Army Engineer Waterways Experiment Station, Vicksburg, Miss., Misc. Paper No. 4-577, June.
- Grant, F. S. and G. F. West (1965). Interpretation Theory in Applied Geophysics, McGraw-Hill, 538 pp.
- Knopoff, L. (1959). "Scattering of Shear Waves by Spherical Obstacles." Geophysics. Vol. 24, pp. 209-219.
- Kolsky, H. (1953). Stress Waves in Solids. Dover Publications. also Clarendon Press, Oxford.
- Lamb, H. (1904). "On the Propagation of Tremors Over the Surface of an Elastic Solid." Philosophical Transactions. Royal Society of London. A., Vol. 203, pp. 1-42.
- Lysmer, J. and F. E. Richart, Jr. (1966). "Dynamic Response of Footings to Vertical Loading." Proc. ASCE. Vol. 22, No. S11, Jan., pp. 65-91.
- Mal, A. K. and L. Knopoff (1965). "Transmission of Rayleigh Waves Past a Step Change in Elevation." Bulletin of the Seismological Society of America. Vol. 55, No. 2, pp. 319-334, April.

- Miller, G. F. and H. Pursey (1955). "On the Partition of Energy Between Elastic Waves in a Semi-Infinite Solid." Proceedings of the Royal Society (London), A. Vol. 233, pp. 55-59.
- Northwood, T. D. and D. V. Anderson (1953). "Model Seismology." Bulletin, Seis. Soc. of Am., Vol. 43, pp. 239-245.
- Oliver, J., F. Press and M. Ewing (1954). "Two-Dimensional Model Seismology." Geophysics. Vol. 19, No. 2, pp. 202-220.
- Tyutekin, V. V. (1959). "Scattering of Plane Waves by a Cylindrical Cavity in an Isotropic Elastic Medium." Soviet Physics-Acoustics. 5, pp. 105-109.
- Viktorov, I. A. (1958). "The Effects of Surface Defects on the Propagation of Rayleigh Waves." Soviet Physics. Doklady, 3, pp. 304-306.
- Woods, R. D. (1967). "Screening of Elastic Surface Waves by Trenches." a dissertation submitted in partial fulfillment of the requirements for the degree of Doctor of Philosophy in the University of Michigan, 160 pp.

APPENDIX II

LIST OF SYMBOLS

G	Shear Modulus
H	Depth of trench (ft)
L	Length of trench (ft)
R	Radial distance from source to straight trench (ft)
R_0	Radial distance from source to circular trench (ft)
W	Width of trench (ft)
P-wave	Compression wave
S-wave	Shear wave
R-wave	Rayleigh wave
c	Cohesion intercept (kg/cm^2)
e	Void ratio
f	Frequency of vibrations (cps)
g	Acceleration of gravity ($32 \text{ ft}/\text{sec}^2$)
k	Ratio, v_R/v_S
r	Radial distance from source of vibrations (ft)
r_0	Radius of footing (ft)
v_P	Velocity of propagation of compression wave (ft/sec)
v_S	Velocity of propagation of shear wave (ft/sec)
v_R	Velocity of propagation of Rayleigh wave (ft/sec)
w	Water content (percent)
θ	Angular length of trench (degrees)
γ	Unit weight (lb/ft^3)
γ_d	Unit weight of dry soil (lb/ft^3)

λ	Lame's constant ($\lambda = \frac{2\nu G}{1 - 2\nu}$)
λ_S	Wave length of shear wave (ft)
λ_R	Wave length of Rayleigh wave (ft)
ν	Poisson's ratio
ρ	Mass density of elastic half space ($\rho = \frac{\gamma}{g}$) (lb-sec ² /ft ⁴)
ϕ	Angle of internal friction (degrees)